

Sequential Stratified Regeneration: *MCMC* for Large State Spaces with an Application to Subgraph Counting Estimation

Carlos H. C. Teixeira¹ · Mayank Kakodkar² · Vinícius Dias^{1,3} · Wagner Meira Jr.¹ · Bruno Ribeiro²

the date of receipt and acceptance should be inserted later

Abstract This work considers the general task of estimating the sum of a bounded function over the edges of a graph that is unknown a priori, where graph vertices and edges are built on-the-fly by an algorithm and the resulting graph is too large to be kept in memory or disk. Prior work proposes Markov Chain Monte Carlo (*MCMC*) methods that simultaneously sample and generate the graph, eliminating the need for storage. Unfortunately, these existing methods are not scalable to massive real-world graphs. In this paper, we introduce Ripple, an *MCMC*-based estimator which achieves unprecedented scalability in this task by stratifying the *MCMC* Markov chain state space with a new technique that we denote *ordered sequential stratified Markov regenerations*. We show that the Ripple estimator is consistent, highly parallelizable, and scales well.

In particular, applying Ripple to the task of estimating connected induced subgraph counts on large graphs, we empirically demonstrate that Ripple is accurate and is able to estimate counts of up to 12-node subgraphs, a task at a scale that has been considered unreachable, not only by prior *MCMC*-based methods, but also by other sampling approaches. For instance, in this target application, we present results where the Markov chain state space is as large as 10^{43} , for which Ripple computes estimates in less than 4 hours on average.

Keywords Markov Chain Monte Carlo, Random Walk, Regenerative Sampling, Motif Analysis, Subgraph Counting, Graph Mining

✉ Carlos H. C. Teixeira

E-mail: carlos@dcc.ufmg.br

¹ Universidade Federal de Minas Gerais, Belo Horizonte, Brazil

² Purdue University, West Lafayette, USA

³ Universidade Federal de Ouro Preto, Ouro Preto, Brazil

1 Introduction

This work considers the following general task (which we later specialize to estimate the number of connected induced subgraphs in large graphs): let $\mathcal{G} = (\mathcal{V}, \mathcal{E})$ be a simple graph, where \mathcal{V} is the set of vertices and \mathcal{E} is the set of edges. A simple graph is a graph that does not contain more than one edge between any two vertices and has no self-loops. Further, assume that \mathcal{G} is *unknown a priori*, such that its vertices and edges are built on-the-fly by an algorithm that, given a node $u \in \mathcal{V}$, is able to determine the set of neighbors of u in \mathcal{G} given by $\mathbf{N}(u) \triangleq \{v \in \mathcal{V} : (u, v) \in \mathcal{E}\}$. However, building the entire graph \mathcal{G} is assumed to be prohibitively expensive.

Our goal is to estimate the sum of a bounded function over all the edges of \mathcal{G} without building and storing the entire graph,

$$\mu(\mathcal{E}) = \sum_{(u,v) \in \mathcal{E}} f(u, v) \quad (1)$$

where $f: \mathcal{E} \rightarrow \mathbb{R}$, $f(\cdot) < B$ is a bounded function for some (possibly very large) constant $B \in \mathbb{R}$. Our main challenge is our inability to directly sample edges in \mathcal{E} , since \mathcal{G} needs to be built on-the-fly and is too large to be stored.

Applications. The above setting is common in the challenging task of counting the number of connected induced subgraphs in some graph G . In these scenarios, \mathcal{G} is a higher-order network (*HON*), where each *HON* edge $(u, v) \in \mathcal{E}$ represents a connected induced k -node subgraph of G such that $u, v \in \mathcal{V}$ represent $(k-1)$ -node subgraphs that share all nodes but one (Wang et al., 2014; Teixeira et al., 2018). We will revisit this application in Section 4.

State-of-the-art large-state-space estimators. The quantity in Equation (1) is generally estimated using specialized Markov Chain Monte Carlo (*MCMC*) estimators. The *MCMC* acts by constructing a random-walk-like Markov chain that has a uniform distribution over the edges \mathcal{E} as its equilibrium distribution. Standard *MCMC* methods are unable to estimate the quantity in Equation (1) and are limited to estimate $\mu(\mathcal{E})/|\mathcal{E}|$, since $|\mathcal{E}|$ in our task is unknown (Ribeiro and Towsley, 2012). The specialized estimators (Avrachenkov et al., 2016) for Equation (1) are practically limited to small graphs \mathcal{G} —based on earlier work for subgraph densities by Bhuiyan et al. (2012a); Wang et al. (2014)—since their running time is $O(|\mathcal{E}|)$.

Traditional *MCMC* methods are limited by their reliance on the Markov chain on \mathcal{G} reaching equilibrium, and chains over large graphs \mathcal{G} tend to take a long time to reach anything close to equilibrium. As a consequence, a significant number of Markov chain steps is needed to *burn in* in order to produce accurate estimates of Equation (1). Parallelism by running multiple Markov chains offers no respite, since parallelism does not reduce the large *burn in* time. Unfortunately, parallelization approaches that divide the state space into disjoint “chunks”, which are to be updated in parallel (Wilkinson, 2006;

Neiswanger et al., 2014), would not work in our setting: Our built-on-the-fly graph \mathcal{G} is unknown to us and may not even have disconnected components that can be parallelized (i.e., disjoint chunks). Currently, *MCMC* on \mathcal{G} is slow and offers no meaningful parallelization opportunities.

Proposed parallelization solution. This work introduces *Sequential Stratified Regeneration* (Ripple), a novel parallel *MCMC* technique that expands the application frontier of *MCMC* to large-state graphs \mathcal{G} . Ripple uses Markov chain regeneration (Nummelin, 1978) and stratifies the underlying Markov chain to break down the problem into a ordered virtual strata. These virtual strata need not be disjoint chunks, rather, they need to be connected. Strata are then processed and estimated one-by-one, in order, using a recursive method, which improves regeneration frequencies and reduces the variance. Ripple offers an unprecedented level of efficiency and parallelism for *MCMC* sampling on built-on-the-fly graphs, while keeping benefits of *MCMC*-based algorithms such as low memory demand (polynomial w.r.t. the output).

Surprisingly, the parallelism of Ripple comes from the regeneration rather than the strata: the strata’s job is to keep regeneration times short. We demonstrate that the estimates obtained by Ripple are consistent, among other theoretical guarantees. Moreover, we empirically show the power of Ripple in a real-world application by estimating subgraph counts of multi-million-node attributed graphs—to the best of our knowledge, a task at a scale that has been thought unreachable by any other *MCMC* sampling method.

Contributions. In addition to the novel regeneration-based *MCMC* algorithm with controllable running times described above, we provide theoretical guarantees for convergence. Our specific contributions to the subgraph counting problem include:

- an end-to-end implementation guide;
- streaming-based optimizations including a parallel reservoir sampling algorithm;
- novel efficiency improvements to the random walk on the *HON* (Wang et al., 2014); and
- a theoretical analysis of scalability in terms of running time and memory w.r.t. the subgraph size, verified empirically on large datasets.

2 Preliminaries

The *MCMC* random-walk-like Markov chain over our built-on-the-fly graph \mathcal{G} is:

Definition 1 (Simple Random Walk on \mathcal{G}) Given a simple graph $\mathcal{G} = (\mathcal{V}, \mathcal{E})$, a simple random walk is a time homogenous Markov chain Φ with state space \mathcal{V} and transition probability

$$p_{\Phi}(u, v) \propto \mathbf{1}_{\{v \in \mathbf{N}(u)\}} / \mathbf{d}(u),$$

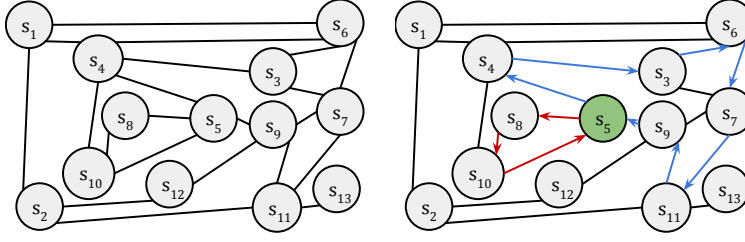


Fig. 1: A simple graph \mathcal{G} (left) and two *RWTs* performed over \mathcal{G} (right) according to Definition 2. Vertex s_5 (green) has been arbitrarily designated as the regeneration point and arrows indicate paths traversed by two *RWTs*, $\mathcal{T} = \{(s_5, s_8, s_{10}), (s_5, s_4, s_3, s_6, s_7, s_{11}, s_9)\}$ marked in red and blue respectively.

where $\mathbf{N}(u) = \{v : (u, v) \in \mathcal{E}\}$ is the neighborhood of u , $\mathbf{d}(u) = |\mathbf{N}(u)|$ is the degree in \mathcal{G} and $\mathbf{1}\{\cdot\}$ is the indicator function.

For the interested reader, Appendix A.1 shows how other *MCMC* tasks over discrete state spaces may be cast into our framework and Appendix A.2 shows the dependence of a simple *MCMC* estimate on the spectral gap $\delta(\Phi)$ and the number of random walk steps.

2.1 Regenerations in Discrete Markov Chains

Since the convergence of standard *MCMC* estimates depends on the spectral gap, practitioners are encouraged to run a single long sample path, which renders them unable to split the task among multiple processors. To overcome this dependence, practitioners use various diagnostics to eyeball if the chain has been mixed (Rosenthal, 1995). However both the mixing time (Diaconis and Stroock, 1991, Prop-3) and the variance of an estimate computed from a mixed chain (Ribeiro and Towsley, 2012) depend on the spectral gap.

Counts, confidence intervals and parallelism. A solution to the above problems is to *split* (Nummelin, 1978) the Markov chain using regenerations. Discrete Markov chains regenerate every time they enter a fixed state which is referred to as a regeneration point. This naturally yields the definition of a *Random Walk Tour* (*RWT*), illustrated in Figure 1.

Definition 2 (*RWT* over Φ) Given a time homogenous markov chain Φ with finite state space \mathcal{V} for some fixed regeneration point $x_0 \in \mathcal{V}$, an *RWT* $\mathbf{X} = (X_i)_{i=1}^\xi$ is a sequence of states visited by Φ such that $X_1 = x_0$ and $|\mathbf{X}| = \xi = \min\{i > 1 : X_{i+1} = x_0\}$, is the first return time to x_0 .

Due to the strong Markov property (Bremaud, 2001, Chap-2, Thm-7.1), *RWTs* from x_0 are i.i.d. and can be used to estimate $\mu(\mathcal{E})$ from Equation (1) when

the volume is unknown (Avrachenkov et al., 2016, 2018; Teixeira et al., 2018; Savarese et al., 2018; Cooper et al., 2016; Massoulié et al., 2006).

Lemma 1 (RWT Estimate) *Given the graph $\mathcal{G} = (\mathcal{V}, \mathcal{E})$, the random walk Φ and the stationary distribution π_Φ from Definition 1, consider $f: \mathcal{E} \rightarrow \mathbb{R}$ bounded by B , and \mathcal{T} , a set of m RWTs started at $x_0 \in \mathcal{V}$ (Definition 2) sampled in a parallel z core environment assuming each core samples an equal number of tours. Then*

$$\hat{\mu}_*(\mathcal{T}; f, \mathcal{G}) = \frac{\mathbf{d}(x_0)}{2m} \sum_{\mathbf{X} \in \mathcal{T}} \sum_{j=1}^{|\mathbf{X}|} f(X_j, X_{j+1}), \quad (2)$$

is an unbiased and consistent estimator of $\mu(\mathcal{E}) = \sum_{(u,v) \in \mathcal{E}} f(u,v)$ if \mathcal{G} is connected, where each X_j refers to the j th state in the RWT $\mathbf{X} \in \mathcal{T}$.

The expected running time for sampling m tours is $O\left(m/z \frac{\text{Vol}(\mathcal{G})}{\mathbf{d}(x_0)}\right)$ and when \mathcal{G} is non bipartite, the variance of the estimate is bounded as

$$\text{Var}(\hat{\mu}_*(\mathcal{T})) \leq \frac{3}{4} \frac{B^2 \text{Vol}(\mathcal{G})^2}{m \delta(\Phi)}, \quad (3)$$

where $\text{Vol}(\cdot)$ and $\delta(\cdot)$ refer to the volume and spectral gap, respectively.

The RWT Estimate can be seen as a transformation of MCMC (Savarese et al., 2018), which takes random time but yields finite sample unbiased estimates of objectives like Equation (1). The parallelism apparent in the expected running time in Lemma 1 emerges directly from the independence of RWTs. Moreover, RWT Estimate's confidence intervals can be computed, since $\sqrt{m} \frac{\hat{\mu}_*(\mathcal{T}) - \mu(\mathcal{E})}{\hat{\sigma}(\mathcal{T})}$ approaches the standard normal distribution for large enough m (Avrachenkov et al., 2016), where $\hat{\sigma}(\mathcal{T})^2$ is the empirical variance of $\hat{\mu}_*(\mathbf{X})$, $\mathbf{X} \in \mathcal{T}$, which is the RWT Estimate computed using individual tours.

Improving regeneration frequency

From Lemma 1 it is clear that increasing the degree of the regeneration point $\mathbf{d}(x_0)$ and the spectral gap $\delta(\Phi)$, and decreasing the volume $\text{Vol}(\mathcal{G})$ leads to reduction in both the variance as well as the running time of the RWT Estimate. Avrachenkov et al. (2016) showed that using the *supernode* in a contracted graph as a regeneration point achieves the above.

Definition 3 (Contracted graph) (Aldous and Fill, 2002; Avrachenkov et al., 2016; Chung and Graham, 1997) Given a graph $\mathcal{G} = (\mathcal{V}, \mathcal{E})$ from Definition 1 and a set of vertices $I \subset \mathcal{V}$, a contracted graph is a multigraph \mathcal{G}_I formed by collapsing I into a single node ζ_I . The vertex set of \mathcal{G}_I is then given by $\mathcal{V} \setminus I \cup \{\zeta_I\}$ and its edge multiset is obtained by conditionally replacing each endpoint of each edge with ζ_I if it is a member of I . We refer to both the set I and the vertex ζ as the supernode.

Contractions benefit *RWTs* since the supernode degree in \mathcal{G}_I , $\mathbf{d}_{\mathcal{G}_I}(\zeta_I)$, and the spectral gap of the random walk on the contracted graph $\delta(\Phi_I)$ increases monotonically with $|I|$ (Avrachenkov et al., 2016) and *RWTs* can be sampled on \mathcal{G}_I without explicit construction, as we see next.

Remark 1 Let the multi-set $\mathbf{N}(\zeta_I) \triangleq \uplus_{u \in I} \mathbf{N}_{\mathcal{G}}(u) \setminus I$ be the neighborhood of the supernode in \mathcal{G}_I as described in Definition 3. Let Φ_I be the simple random walk on \mathcal{G}_I . An *RWT* $(X_i)_{i=1}^\xi$ on Φ_I where $X_1 = \zeta_I$, can be built by sampling X_2 u.a.r. from $\mathbf{N}(\zeta_I)$ and by sampling subsequent transitions according to Φ till the chain enters I . That is, $\xi = \min\{i > 1 : X_{\xi+1} \in I\}$.

There is however a trade-off.

Remark 2 To compute the number of edges coming out of the supernode ζ_I in \mathcal{G}_I , $\mathbf{d}_{\mathcal{G}_I}(\zeta_I) = |\mathbf{N}(\zeta_I)|$, and to sample from $\mathbf{N}(\zeta_I)$ in order to start the *RWT*, we need to enumerate the set of the edges incident on I in \mathcal{G} given by $\mathcal{E}_* \subset \mathcal{E}$.

As such, a massive supernode I could make the cost of enumerating \mathcal{E}_* prohibitively large and hinder the utility of the above construction in extremely large state spaces that require large supernodes. However, the stratification of \mathcal{E} into \mathcal{E}_* and $\mathcal{E} \setminus \mathcal{E}_*$ provides a way to decompose the task of estimating $\mu(\mathcal{E})$ as $\mu(\mathcal{E}_*) + \mu(\mathcal{E} \setminus \mathcal{E}_*)$, where we can exactly compute the first term and estimate the second using the *RWT* Estimate on the contracted graph (detailed in Section 3.3). This last observation motivates our method.

3 Sequential Stratified Regenerations

Increasing the size of the supernode ζ in the collapsed graph \mathcal{G}_I encourages faster regenerations, specially in large state spaces, but it also makes the exact computation of the number of supernode edges $\mathbf{d}_{\mathcal{G}_I}(\zeta)$ prohibitively expensive (see Remark 2). Next we describe how to get around this trade-off with our method Ripple’s *sequential stratification*.

Ripple controls regeneration times through a *sequential stratification* of the state space of the Markov chain. After stratifying the vertices and edges of \mathcal{G} into ordered strata, we build, for each stratum, a graph with a supernode that consists of all prior strata. *RWTs* are then performed over each *graph stratum*, considering the supernodes as regeneration points. Thus, Ripple controls the volume of the Markov chain graph while improving the degree of the regeneration point and the spectral gap. This directly improves regeneration frequency and reduces the variance of the *RWT* Estimate as shown in Lemma 1.

A crucial impediment here is the exact computation within the supernode as pointed out by Remark 2. We overcome this impediment through a recursive procedure that approximates the random walker at the supernode using tours in the previous strata. We show that such approximation doesn’t preclude parallelism and the ability to compute confidence intervals, both being innate qualities of regenerative sampling as described in Section 2.1. Finally, we show that the bias introduced by this approximation asymptotically converges to

zero as the number of tours increase, and therefore yields a consistent estimator (asymptotically unbiased).

For the subgraph sampling problem covered in Section 4 we show, in Proposition 6, that the total number of random walk steps performed is linear in the diameter and maximum degree of the input graph and cubic in the subgraph size. We further show that Ripple’s time and space complexity are polynomial in terms of the subgraph size.

3.1 Sequential Stratification

First we define a simple method to stratify vertices and edges of any graph \mathcal{G} into R disjoint partitions.

Definition 4 (Sequential Stratification) Given $\mathcal{G} = (\mathcal{V}, \mathcal{E})$ from Definition 1, a function $\rho: \mathcal{V} \rightarrow \{1, \dots, R\}$ is said to induce the stratification $(\mathcal{I}_r, \mathcal{J}_r)_{r=1}^R$ if $s \in \mathcal{I}_{\rho(s)}$, for each $s \in \mathcal{V}$, and $(u, v) \in \mathcal{J}_{\min(\rho(u), \rho(v))}$, for each $(u, v) \in \mathcal{E}$.

It is easy to see that the strata are pairwise disjoint and their union yields the vertex set and edge set of the graph. Next, we describe the contracted graph over which *RWTs* are to be sampled in each stratum.

Definition 5 (*r*-th Graph Stratum) Let $\mathcal{A}_{i:j} \triangleq \mathcal{A}_i \cup \mathcal{A}_{i+1} \cup \dots \cup \mathcal{A}_j$ be defined for any ordered tuple of sets. Let $(\mathcal{I}_r, \mathcal{J}_r)_{r=1}^R$ be the stratification induced by ρ from Definition 4 on $\mathcal{G} = (\mathcal{V}, \mathcal{E})$. The *r*-th graph stratum $\mathcal{G}_r = (\mathcal{V}_r, \mathcal{E}_r)$, $r > 1$, is obtained by

- contracting $\mathcal{I}_{1:r-1}$ into ζ_r according to Definition 3,
- and then removing all edges not incident on $\mathcal{I}_{1:r}$ and vertices that do not share an edge with vertices in $\mathcal{I}_{1:r}$.

Further, let Φ_r denote the simple random walk on \mathcal{G}_r .

It can be shown that the vertex set \mathcal{V}_r contains the *r*-th stratum \mathcal{I}_r , the *r*-th supernode ζ_r , obtained by collapsing all vertices in $\mathcal{I}_{1:r-1}$, and vertices from subsequent strata neighboring \mathcal{I}_r , $\cup_{u \in \mathcal{I}_r} \mathbf{N}(u) \cap \mathcal{I}_{r+1:R}$. Also, the edge multiset \mathcal{E}_r is the union of \mathcal{J}_r and edges that connect ζ_r to vertices in \mathcal{I}_r , which are a result of the graph contraction in Definition 5. We present a detailed example of this procedure in Figure 2.

Note that a special case arises when $R = 2$ with \mathcal{G}_2 graph stratum. In such scenario our estimator – introduced in Definition 9 – reduces to the estimator from Avrachenkov et al. (2016). In addition to generalize the latter, we provide an alternate proof for ignoring self loops in the supernode when sampling *RWTs* in Appendix A.3.

3.2 Ergodicity-Preserving Stratification (*EPS*)

Since Lemma 1 postulates that the *RWT* Estimate is consistent only if the underlying graph is connected, we have:

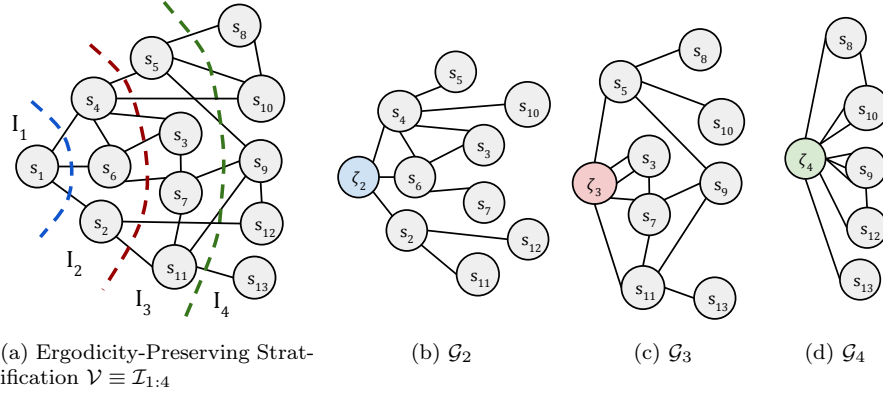


Fig. 2: Figure 2a shows a simple graph \mathcal{G} that is stratified into four strata $\{\mathcal{I}_1, \mathcal{I}_2, \mathcal{I}_3, \mathcal{I}_4\}$. Figures 2b to 2d show the second, third and fourth graph strata respectively, constructed according to Definition 5. Note in Figure 2b how, in \mathcal{G}_2 which is a multi-graph, vertices in \mathcal{G}_1 are collapsed into ζ_2 and only edges incident on \mathcal{I}_2 are preserved. The edge set therefore contains \mathcal{J}_2 and the edges between ζ_2 and \mathcal{I}_2 . Consequently, self loops on ζ_2 and edges between $\mathcal{I}_{3:4}$ are absent. Figures 2c and 2d follow suit.

Definition 6 (Ergodicity-Preserving Stratification (EPS)) The function ρ from Definition 4 is said to yield an Ergodicity-Preserving Stratification, if the r -th graph stratum from Definition 5 is connected, which implies that Φ_r is irreducible, for each $r > 1$.

We propose necessary and sufficient conditions on ρ that lead to an EPS.

Proposition 1 ρ yields an EPS if the following three conditions are satisfied:

- (a) for at least one vertex in each connected component of \mathcal{G} , ρ evaluates to 1;
- (b) for each u : $\rho(u) = r$, there exists $v \in \mathbf{N}(u)$ such that $\rho(v) \leq r$; and
- (c) there exists $(u_0, v_0) \in \mathcal{E}$, such that $\rho(u_0) = r$ and $\rho(v_0) < r$.

In practice, lower bounds for the fraction of vertices in \mathcal{I}_r connected to $\mathcal{I}_{1:r-1}$ can be used to upper bound expected return times to the supernode, a fact we use in Proposition 6.

3.3 Per-Stratum Regenerations

In order to explain our recursive sampling algorithm over the ergodicity-preserving stratification, we first start with an oversimplified version of our algorithm. Here, we will unrealistically assume that we know the strata degrees, $\mathbf{d}(\zeta_r)$, $r = 2, \dots, R$, and we can perfectly sample outgoing edges of a supernode ζ_r according to the random walk transition probability $p_{\Phi_r}(\zeta_r, \cdot)$ out of the supernode ζ_r . Later we will remove these assumptions.

Assumption 1 Assume in each graph stratum \mathcal{G}_r , $r = 2, \dots, R$, that the degree of the supernode $\mathbf{d}(\zeta_r)$ is known and the random walk transition probability out of ζ_r given by $p_{\Phi_r}(\zeta_r, \cdot)$ can be sampled from.

Under Assumption 1, RWTs can be sampled in each stratum as follows.

Proposition 2 (RWTs in Φ_r) Given access to the chain Φ and the stratifying function ρ , let Φ_r be the random walk in the r -th graph stratum \mathcal{G}_r from Definition 5. The procedure to sample an RWT $(X_i)_{i=1}^\xi$ over Φ_r originating at the supernode ζ_r starts by setting $X_1 = \zeta_r$ and sampling $X_2 \sim p_{\Phi_r}(\zeta_r, \cdot)$. Subsequently, we sample

$$X_{i+1} \sim \begin{cases} \text{UNIF}(\mathbf{N}_{\mathcal{G}}(X_i)) & \text{if } \rho(X_i) = r \\ \text{UNIF}(\mathbf{N}_{\mathcal{G}}(X_i) \cap \mathcal{I}_r) & \text{if } \rho(X_i) > r \end{cases}$$

till $\rho(X_{\xi+1}) < r$, i.e., ξ is the hitting time of the supernode $\mathcal{I}_{1:r-1}$.

Per-stratum estimates can then be computed using such RWTs as:

Proposition 3 (Perfectly Stratified Estimate) Under Assumption 1, given the graph stratum \mathcal{G}_r (Definition 5), a bounded function $f: \mathcal{E} \rightarrow \mathbb{R}$ and a set of m RWTs \mathcal{T}_r sampled over Φ_r with origin ζ_r according to Proposition 2, the per stratum estimate

$$\hat{\mu}(\mathcal{T}_r; f, \mathcal{G}_r) = \frac{\mathbf{d}(\zeta_r)}{2m} \sum_{\mathbf{X} \in \mathcal{T}_r} \sum_{j=2}^{|\mathbf{X}|-1} f(X_j, X_{j+1}), \quad (4)$$

where X_j is the j th state visited in the RWT $\mathbf{X} \in \mathcal{T}_r$, is an unbiased and consistent estimator of the edge sum over the r -th edge stratum (Definition 4) $\mu(\mathcal{J}_r) = \sum_{(u,v) \in \mathcal{J}_r} f(u, v)$ for all $r > 1$.

Proposition 3 applied on each stratum yields $\mu(\mathcal{J}_1) + \sum_{r=2}^R \hat{\mu}_r(\mathcal{T}_r)$, the unbiased estimate of $\mu(\mathcal{E}) = \sum_{r=1}^R \mu(\mathcal{J}_r)$ in Equation (1). Next, we modify the above algorithm to remove the need for Assumption 1.

3.4 Towards Tractability Through Recursion

Assumption 1 is unrealistic for $R > 2$, specially for a large-state graph which needs to be built on-the-fly. We therefore propose using estimates of the supernode degree $\mathbf{d}(\zeta_r)$ and the transition probability $p_{\Phi_r}(\zeta_r, \cdot)$, rather than their true values.

Definition 7 (Supernode Estimates, $\hat{\mathbf{d}}(\zeta_r)$ and $\hat{p}_{\Phi_r}(\zeta_r, \cdot)$) Given a stratification of \mathcal{G} , the supernode estimates in the r -th graph stratum \mathcal{G}_r consist of the estimate of the degree $\hat{\mathbf{d}}(\zeta_r)$ and a sample from an approximate transition probability out of the supernode $\hat{p}_{\Phi_r}(\zeta_r, \cdot)$. We let $\hat{\Phi}_r$ be the Markov chain with transition probabilities equal to the random walk Φ_r on \mathcal{G}_r everywhere, except at the supernode where transitions are sampled from $\hat{p}_{\Phi_r}(\zeta_r, \cdot)$.

Trivially, Proposition 3 only holds in the ideal case, when $\hat{\mathbf{d}}(\zeta_r) = \mathbf{d}(\zeta_r)$ and $\hat{p}_{\Phi_r}(\zeta_r, \cdot) \equiv p_{\Phi_r}(\zeta_r, \cdot)$. But, as we later show, the bias introduced due to the use of estimates instead of exact quantities in Theorem 2 can be quantified.

Although $\hat{\Phi}_r$ may not be reversible, *RWTs* on $\hat{\Phi}_r$ retain the renewal property. Such tours are hence pairwise independent and preserve the benefits stated at the end of Section 2.1. This motivates a recursive solution that makes use of *supernode estimates* and tours sampled in the previous strata to compute the supernode estimates in the current stratum, as shown next.

Definition 8 (Ripple’s Recurrence Relation) Given a stratification of the graph \mathcal{G} according to Definition 6, let r be some stratum where $1 < r \leq R$. Assume that the previous steps of the recursion have completed and, therefore, for all $2 \leq q < r$, a set of m_q *RWTs* (\mathcal{T}_q^\dagger) have been sampled. Conditioned on such tours, we’re given the supernode degree estimates $\hat{\mathbf{d}}(\zeta_q)$ and estimated transition probabilities out of the supernode $\hat{p}_{\Phi_q}(\zeta_q, \cdot)$.

Let the estimate of the number of edges between \mathcal{I}_q and \mathcal{I}_r be given by

$$\hat{\beta}_{q,r} = \frac{\hat{\mathbf{d}}(\zeta_q)}{|\mathcal{T}_q^\dagger|} \sum_{\mathbf{X} \in \mathcal{T}_q^\dagger} \sum_{j=2}^{|\mathbf{X}|} \mathbf{1}\{\rho(X_j) = r\}, \quad (5)$$

where X_j is the j -th state visited in tour \mathbf{X} . By convention, we assume that $\hat{\beta}_{1,r} = \sum_{u \in \mathcal{I}_1} \sum_{v \in \mathbf{N}(u)} \mathbf{1}\{\rho(v) = r\}$ is exactly computed.

The degree estimate of the supernode in the r -th stratum is then given by

$$\hat{\mathbf{d}}(\zeta_r) = \sum_{q=1}^{r-1} \hat{\beta}_{q,r}, \quad (6)$$

and transitions according to $\hat{p}_{\Phi_r}(\zeta_r, \cdot)$ are sampled by sampling $q \in \{1, \dots, r-1\}$ with probability (w.p.) proportional to $\hat{\beta}_{q,r}$. Then, sampling u.a.r. from $\hat{\mathbf{U}}_{q,r}$ is defined as

$$\hat{\mathbf{U}}_{q,r} = \begin{cases} \uplus_{\mathbf{X} \in \mathcal{T}_q^\dagger} \uplus_{j=2}^{|\mathbf{X}|} \{X_j : \rho(X_j) = r\}, & \text{if } q > 1, \\ \uplus_{u \in \mathcal{I}_1} \{v \in \mathbf{N}(u) : \rho(v) = r\}, & \text{if } q = 1, \end{cases} \quad (7)$$

where \uplus is the multi-set union, and $\hat{\mathbf{U}}_{q,r}$, $q > 1$, is the multi-set union of all states in \mathcal{I}_r visited by the random walk on $\hat{\Phi}_q$, whereas $\hat{\mathbf{U}}_{1,r}$ are neighbors of vertices in the first stratum which lie in \mathcal{I}_r . Thus, we may relax Proposition 2 considering the transition probability $\hat{p}_{\Phi_r}(\zeta_r, \cdot)$ to sample tours \mathcal{T}_r^\dagger in the r -th stratum.

Thus, using the supernode estimates computed and tours sampled recursively in Definition 8, $\mu(\mathcal{E})$ of Equation (1) can be estimated by adapting Proposition 3, as follows.

Definition 9 (Ripple's μ Estimator) Given the graph strata \mathcal{G}_r , $2 \leq r \leq R$ from an Ergodicity-Preserving Stratification of \mathcal{G} from Definition 6, let $\widehat{\mathbf{d}}(\zeta_r)$ be the supernode degree estimate and \mathcal{T}_r^\dagger be the random walk tours sampled in each stratum using Definition 8. The Ripple estimate is then given by

$$\hat{\mu}_{\text{Ripple}} = \mu(\mathcal{J}_1) + \sum_{r=2}^R \hat{\mu}(\mathcal{T}_{2:r}^\dagger; f), \quad (8)$$

such that

$$\hat{\mu}(\mathcal{T}_{2:r}^\dagger; f) = \frac{\widehat{\mathbf{d}}(\zeta_r)}{2|\mathcal{T}_r^\dagger|} \sum_{\mathbf{X} \in \mathcal{T}_r^\dagger} \sum_{j=2}^{|\mathbf{X}|-1} f(X_j, X_{j+1}), \quad (9)$$

where X_j is the j th state visited by the RWT $\mathbf{X} \in \mathcal{T}_r^\dagger$ and $\widehat{\mathbf{d}}(\zeta_r)$ depends on the tours in the previous strata, $\mathcal{T}_{2:r-1}^\dagger$.

Theorem 1 *The Ripple estimate from Definition 9 is a consistent estimator of $\mu(\mathcal{E})$ (asymptotically unbiased in the number of tours), that is,*

$$\lim_{|\mathcal{T}_2^\dagger| \rightarrow \infty} \dots \lim_{|\mathcal{T}_R^\dagger| \rightarrow \infty} \mu(\mathcal{J}_1) + \sum_{r=2}^R \hat{\mu}(\mathcal{T}_{2:r}^\dagger; f) \stackrel{a.s.}{=} \mu(\mathcal{E}).$$

When the number of tours is finite, then the Ripple estimate is biased. We see that this bias depends on the bias in the supernode estimates ($\widehat{\mathbf{d}}(\zeta_r)$ and $\widehat{p}_{\Phi_r}(\zeta_r, \cdot)$), as follows.

Theorem 2 *Assuming that each EPS stratum \mathcal{G}_r from Definition 5 is connected and non bipartite, let $\widehat{\mathbf{d}}(\zeta_r)$ and $\widehat{p}_{\Phi_r}(\zeta_r, \cdot)$ be the estimate of the degree and transition probability at the supernode and let Φ_r be the random walk on \mathcal{G}_r . The bias of the Ripple estimate in the r th stratum from Equation (9) is then given by*

$$\left| \mathbb{E} \left[\hat{\mu}(\mathcal{T}_{2:r}^\dagger; f) \mid \mathcal{T}_{2:r-1}^\dagger \right] - \mu(\mathcal{J}_r) \right| \leq (\lambda_r \nu_r + |1 - \lambda_r|) \frac{\sqrt{3}B|\mathcal{E}_r|}{\sqrt{\delta_r}},$$

where δ_r is the spectral gap of Φ_r , B is the upper bound of f , $\nu_r = \|\widehat{p}_{\Phi_r}(\zeta_r, \cdot) - p_{\Phi_r}(\zeta_r, \cdot)\|_2$ is the L^2 distance between transition probabilities out of ζ_r ((Al-dous and Fill, 2002, Sec 2.4.2), Definition 14) and $\lambda_r = \widehat{\mathbf{d}}(\zeta_r)/\mathbf{d}(\zeta_r)$.

Therefore, the bias in subsequent EPS strata depends crucially on the bias in the current stratum. Motivated by this fact, in practice one should attempt to control the empirical variance in each stratum by appropriately increasing the number of tours sampled (in our application of choice, this approach is detailed in Section 4.5, Remark 3).

In the next section we provide a concrete implementation of Ripple to estimate subgraph counts on large graphs.

4 Application of Ripple to Subgraph Counting

We focus on applying Ripple to the task of counting subgraphs given an undirected, attributed, finite and simple graph $G = (V, E, L)$ with vertices V , edges E , and attribute function L . We start by defining what we are counting, connected induced subgraphs:

Definition 10 (Connected Induced Subgraph (CIS)) Let $G(V') = (V', E \cap (V' \times V'), L)$ be the subgraph induced by any $V' \subset V$ on G . $G(V')$ is referred to as a Connected Induced Subgraph (CIS) of size k or k -CIS when it is connected and $|V'| = k$.

In what follows, we rarely talk about disconnected subgraphs, unless specified, a *subgraph* is understood to be a CIS. Next we define the subgraph pattern count problem.

Definition 11 (Subgraph pattern count) Let $\mathcal{V}^{(k)}$ denote the set of all k -CISs of a graph G and let \sim denote the graph isomorphism equivalence relation (or any equivalence relation) and let \mathcal{H} be an arbitrary set of pairwise non equivalent k -CISs. The subgraph pattern count is defined as the $|\mathcal{H}|$ -dimensional vector $\mathcal{C}^{(k)} = (\mathcal{C}_H^{(k)})_{H \in \mathcal{H}}$, where $\mathcal{C}_H^{(k)} = \sum_{s \in \mathcal{V}^{(k)}} \mathbf{1}\{s \sim H\}$, and $\mathbf{1}\{\cdot\}$ is the indicator function.

Therefore, $\mathcal{C}^{(k)}$ contains the number of subgraphs in $\mathcal{V}^{(k)}$ that are equivalent to each pattern in \mathcal{H} and the dependence of $\mathcal{C}^{(k)}$ on \mathcal{H} is suppressed to simplify notation.

Roadmap (applying Ripple for CIS counting):

- We reduce the subgraph counting problem to an edge sum (Equation (1)) over a *HON* graph, as defined in Section 4.1.
- An Ergodicity-Preserving Stratification for the simple random walk on the *HON* is then defined in Section 4.2.
- In Section 4.3 we exploit streaming algorithms to render the memory requirement of our algorithm invariant to the count and the length of tours.
- Finally, we speed up random walks on the aforementioned *HON* through a novel rejection sampling algorithm described in Section 4.4.

While the graph over which we sample random walks and compute the edge sums (later defined as the *HON*) is an unweighted simple graph, the core underlying principles can very easily be extended to arbitrary weighted graphs.

4.1 MCMC on the Subgraph Space

In large and sparse graphs, for a reasonably large k , enumerating $\mathcal{V}^{(k)}$ is not tractable. Since the set of all k -CISs of a graph G , $|\mathcal{V}^{(k)}|$, is much smaller than all possible induced k -node subgraphs, $\binom{|V|}{k}$, the probability of obtaining a CIS from naively independent sampled vertices is very low. To enable a random walk based solution, Wang et al. (2014) proposed creating a network over subgraphs called the *HON*, defined next.

Definition 12 (Higher Order Network (k -HON) (Wang et al., 2014))

The Higher Order Network or *HON* $\mathcal{G}^{(k)} = (\mathcal{V}^{(k)}, \mathcal{E}^{(k)})$ is a graph whose vertices are given by $\mathcal{V}^{(k)}$, the set of all k -CIS contained in graph G , and edges such that $(u, v) \in \mathcal{E}^{(k)}$ if they share all but $k - 1$ vertices, that is $|V(u) \cap V(v)| = k - 1$.

Since the subgraph induced by the union of vertices in u and v , where $(u, v) \in \mathcal{E}^{(k)}$, is a $k + 1$ node subgraph, we use the $k - 1$ -HON to sample k node subgraphs. The *HON* is unknown a priori and therefore its vertices and edges are built on-the-fly as the random walker reaches them. We show in Section 4.4 how this can be done efficiently. The subgraph counts $\mathcal{C}^{(k)}$ from Definition 11 can then be written as an edge sum over the edges of $\mathcal{G} \equiv \mathcal{G}^{(k-1)}$ as

$$\mathcal{C}^{(k)} = \mu(\mathcal{E}^{(k-1)}) = \sum_{(u,v) \in \mathcal{E}^{(k-1)}} \left(\frac{\mathbf{1}\{G(V(u) \cup V(v)) \sim H\}}{\gamma(u,v)} \right)_{H \in \mathcal{H}}, \quad (10)$$

where $\gamma(u, v) = |\{(\ddot{u}, \ddot{v}) \in \mathcal{E} : V(u) \cup V(v) \equiv V(\ddot{u}) \cup V(\ddot{v})\}|$ is the number of edges which represent the exact same subgraph as (u, v) . The edges sampled by a random walk on $\mathcal{G}^{(k-1)}$ is called the *Pairwise Subgraph Random Walk* (PSRW).

4.2 Ergodicity-Preserving Stratification (EPS) for Subgraph Counting

Towards using the Ripple estimator, we first define the function ρ , which stratifies the HON \mathcal{G} according to Definition 4. Computing ρ needs to be efficient since it is evaluated at each step of the random walk and the Ripple estimators from Definitions 8 and 9 heavily depend on it.

Proposition 4 (EPS for subgraphs) *Consider the set of n_1 seed subgraphs \mathcal{I}_1 such that no two subgraphs in \mathcal{I}_1 share a vertex in G and let $V(\mathcal{I}_1) \triangleq \cup_{\check{s} \in \mathcal{I}_1} V(\check{s})$ be the set of all vertices forming subgraphs in \mathcal{I}_1 . For each vertex $u \in V$, let $\text{DIST}(u)$ be the length of the shortest path from u to any vertex in $V(\mathcal{I}_1)$. Define $\rho: \mathcal{S}^{(k-1)} \rightarrow \{1, \dots, R\}$ as*

$$\rho(s) = 1 + \sum_{u \in V(s)} (\text{DIST}(u) + \mathbf{1}\{u \in V(\mathcal{I}_1) \setminus V^*\}),$$

where V^* is the largest connected subset of $V(s)$ such that $V^* \subseteq V(\check{s})$ for some seed vertex $\check{s} \in \mathcal{I}_1$ with ties broken arbitrarily. If \mathcal{I}_1 contains a subgraph from each connected component of G , the stratification from Definition 4 generated using ρ is an *Ergodicity-Preserving Stratification* (Definition 6).

It is easy to see that DIST can be precomputed for all $u \in V$ using a single BFS in $O(|V| + |E|)$ and ρ can be computed in $O(k)$. While R is unknown a priori it is upper bounded as $(k - 1) \cdot D_G$, where D_G is the diameter of G . As the algorithm progresses, *empty* strata, i.e., strata where the estimated degree of the supernode $\mathbf{d}(\zeta_r) = 0$, are simply ignored. In practice, to control the

bias propagation from Theorem 2, we reduce the number of non empty strata significantly by including subgraphs in \mathcal{I}_1 which are far apart in G effectively reducing $\max_{u \in V} \text{DIST}(u)$.

4.3 Memory-Efficiency through Streaming Algorithms

The recurrence relationship from Definition 8 essentially uses recursively sampled tours in the r -th stratum \mathcal{T}_r^\dagger to compute $\hat{\mu}(\mathcal{T}_{2:r}^\dagger; f)$, the estimate of $\mu(\mathcal{J}_r)$. Concurrently, for all $t > r$, we estimate the size of and sample from the set of vertices in \mathcal{I}_t connected to \mathcal{I}_r , given respectively by $\hat{\beta}_{r,t}$ and $\hat{\mathbf{U}}_{r,t}$. Although $\hat{\mu}(\mathcal{T}_{2:r}^\dagger; f)$ and $\hat{\beta}_{r,t}$ can be computed in a streaming fashion over tours with constant memory per thread, $|\hat{\mathbf{U}}_{r,t}|$ may demand a significant amount of memory. If implemented naively, the number of states we need to keep in memory would be the sum of lengths of all tours in each stratum. This restricts the utility of Ripple due to both, the randomness in the tour length and the number of tours required to be sampled to reduce variance.

We address this restriction using *Algorithm R* (Vitter, 1985), which enables a practitioner to sample without replacement, a fixed set of elements uniform at random from a stream of unknown length. In essence, for a fixed pair of strata $r < t$, we replace the uniform distribution $\hat{\mathbf{U}}_{r,t}$, i.e., states in the t -th stratum visited by tours in the r -th stratum \mathcal{G}_r with a uniformly drawn sample of fixed size. This procedure introduces a hyperparameter M , which allows control over the memory requirement at the expense of increasing bias. It is trivial to note that if, for some stratum, the number of tours $|\mathcal{T}_r^\dagger| > M$, the error increases due to (possible) oversampling, which we empirically observe in Figure 5 (Section 5). Next, we detail our low-contention, parallel implementation of which samples $\hat{\mathbf{U}}_{r,t}$, for all $2 \leq r < t \leq R$.

Parallel sampling with a Reservoir Matrix. Given a reasonably large M , and the number of strata R , we initialize an upper triangular matrix of empty reservoirs $[\hat{\mathbf{U}}_{r,t}]_{2 \leq r < t \leq R}$ and a matrix of atomic counters $[\hat{M}_{q,r}]_{2 \leq r < t \leq R}$ initialized to 0. In the stratum r , we sample tours in parallel and whenever the tour enters the t -th stratum, $\hat{M}_{r,t}$ is incremented. With a probability $\min(1, M/\hat{M}_{r,t})$ the state is inserted into a random position in the reservoir $\hat{\mathbf{U}}_{r,t}$ and rejected otherwise. As such, the only contention between threads is at the atomic counter and in the extremely rare case where two threads decide to overwrite the exact same location in the reservoir. Ties are broken based on the value of the atomic counter at the time the decision to insert is made, guaranteeing thread-safety. The space complexity of a reservoir matrix is therefore $O(R^2M)$.

A toy example of the reservoir matrix is presented in Figure 3, where $R = 5$, and the *RWTs* are being sampled on the graph stratum \mathcal{G}_2 from the supernode ζ_2 (represented in black). Whenever (non-gray) states in $\mathcal{I}_{3:5}$ are visited, they're inserted into the corresponding reservoirs – the reservoir for $\hat{\mathbf{U}}_{2,5}$ is depicted in detail.

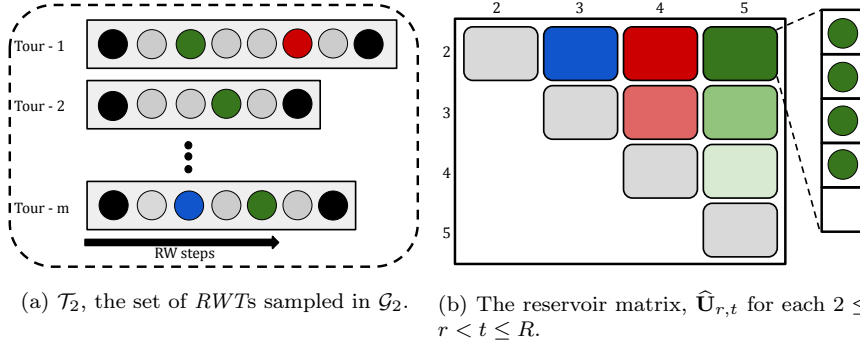


Fig. 3: Parallel RWT s and Reservoirs: Figure 3a shows the set of m RWT s sampled on \mathcal{G}_2 in parallel, where the supernode ζ_2 is colored black. The gray, blue, red and green colors represent states in stratum 2, 3, 4, and 5 respectively. Figure 3b shows the upper triangular matrix of reservoirs where the cell in the r -th row and t -th column contains the reservoir with samples from $\hat{\mathbf{U}}_{r,t}$.

4.4 Speeding up Random Walks in $\mathcal{G}^{(k-1)}$

The neighborhood of a subgraph s in $\mathcal{G}^{(k-1)}$ can be represented as a set of all vertices u and v such that removing u from s and adding v yields a CIS of the same size. Formally,

$$\mathbf{N}_{\mathcal{G}^{(k-1)}}(s) \equiv \left\{ (u, v) \in V(s) \times \mathbf{N}_G(V(s)) : G(V(s) \cup \{v\} \setminus \{u\}) \in \mathcal{V}^{(k-1)} \right\}, \quad (11)$$

where $\mathbf{N}_G(V(s)) = \cup_{x \in V(s)} \mathbf{N}_G(x)$ is the union of the neighborhood of each vertex in s . The size of the neighborhood is then $O(k \mathbf{N}_G(V(s)))$ and the connectivity check requires as many graph traversals (BFS or DFS).

A brute force algorithm would therefore take $O(k^4 \Delta_G)$ operations to enumerate $\mathbf{N}_{\mathcal{G}}(s)$ for a given subgraph s since $\mathbf{N}_G(V(s)) \in O(k \Delta_G)$, where Δ_G is the maximum degree in G .

Fast neighbor selection via rejection sampling. In Algorithm 1, we propose a novel rejection sampling algorithm that samples uniformly from $\mathbf{N}_{\mathcal{G}^{(k-1)}}(s)$, while minimizing the number of graph traversals. To aid efficiency, we use Hopcroft and Tarjan (1973)'s *Articulation Point* algorithm (Appendix A.4), which enumerates the vertices of a graph whose removal disconnects the graph using a single DFS.

Proposition 5 *Given the subgraph $s \in \mathcal{V}^{(k-1)}$, Algorithm 1 samples a neighbor from $\mathbf{N}(s)$ uniformly at random in $O(k^2 \frac{\Delta_s + k|\mathcal{A}_s|}{k - |\mathcal{A}_s|})$ expected time, where $\Delta_s \triangleq \max_{u \in V(s)} \mathbf{d}_G(u)$ is the maximum degree among vertices in s and \mathcal{A}_s is the set of articulation points of s .*

Algorithm 1: Efficient Neighborhood Sampling in $\mathcal{G}^{(k-1)}$

Input: $k-1$ -CIS s , Graph G
Output: $x \sim \text{UNIF}(\mathbf{N}_{\mathcal{G}^{(k-1)}}(s))$

```

1 Let  $\deg_s = \sum_{u \in V(s)} \mathbf{d}(u)$ 
2 Let  $\mathcal{A}_s$  be the set of articulating points of  $s$  from Appendix A.4
3 while True do
4   Sample  $u$  from  $V(s)$  w.p.  $\propto \deg_s - \mathbf{d}(u)$  ;           // Sample a vertex to remove
5   Sample  $a$  from  $V(s) \setminus \{u\}$  w.p.  $\propto \mathbf{d}(a)$ 
6   Sample  $v \sim \text{UNIF}(\mathbf{N}(a))$  ;                               // Sample a vertex to add
7   /* Rejection test */
8   BIAS =  $|N(v) \cap V(s) \setminus \{u\}|$  ;                       // Computing  $v$ 's bias
9   if  $\text{UNIF}(0, 1) \leq 1/\text{BIAS}$  then
10     $x = G(V(s) \cup \{v\} \setminus \{u\})$ 
11    if  $u \neq v$  and  $(u \notin \mathcal{A}_s \text{ or } x \text{ is connected})$  then
12      return  $x$  ;                                           // Connectivity Check
13  continue ;                                               // Reject

```

Therefore, Algorithm 1 has a running time $\in O(k\Delta_s + k^2)$ when s is dense (i.e., $|\mathcal{A}_s| \approx 0$). For sparse subgraphs, the complexity increases to $O(k^2\Delta_s + k^4)$, which is still faster than the naive algorithm.

4.5 The Ripple k -CIS Count Estimator Algorithm

We now summarize the entire procedure to compute the Ripple k -CIS count estimator in Algorithm 2. Ripple's parameters include \mathcal{I}_1 , the set of subgraphs in the initial stratum and the reservoir size limit M . Additionally, Ripple requires, as input, the Per-Stratum Error Bound or Error Bound for short ϵ , which is used to decide the number of *RWTs* that need to be sampled in each stratum.

Remark 3 In each stratum r , given the partition error bound ϵ , *RWTs* are sampled till we satisfy

$$\hat{\sigma}(\mathcal{T}_r^\dagger; f_1) / \sqrt{|\mathcal{T}_r^\dagger|} \leq \epsilon \hat{\mu}(\mathcal{T}_r^\dagger; f_1), \quad (12)$$

where $f_1(\cdot) = 1$ is a constant valued function, $\hat{\mu}(\mathcal{T}_r^\dagger; f_1)$ is the Ripple estimate from Equation (9) of the number of edges in the r -th graph stratum \mathcal{G}_r and $\hat{\sigma}^2(\mathcal{T}_r^\dagger; f_1) = \widehat{\text{Var}}_{\mathbf{X} \sim \mathcal{T}_r^\dagger}(\hat{\mu}(\mathbf{X}; f_1))$ is the former's empirical variance over tours.

Clearly, as ϵ goes to 0, the required number of tours tends to ∞ and the Ripple estimate converges to the ground truth, as described in Theorem 1. We also show that the running time and memory requirement of the Ripple algorithm is polynomial in k . Ignoring the time and space required to load the input graph into memory, both the time and memory are invariant to the number of vertices and edges of the original graph G and depend only on the diameter and maximum degree of G .

Proposition 6 *We assume a constant number of tours m in each stratum and ignore graph loading. The Ripple Estimator of k -CIS counts described in Algorithm 2 has space complexity in*

$$O(k^3 D_G^2 M + |\mathcal{H}|) \equiv \hat{O}(k^3 + |\mathcal{H}|),$$

where \hat{O} ignores all factors other than k and $|\mathcal{H}|$, M is the size of the reservoir from Section 4.3, D_G is the diameter of G and $|\mathcal{H}|$ is the number of patterns of interest.

The total number of random walk steps is given by $O(k^3 m D_G \Delta_G C_{\text{REJ}})$, where C_{REJ} is the number of rejections in Line 21 of Algorithm 2 and Δ_G is the largest degree in G and the total time complexity is $\hat{O}(k^7 + |\mathcal{H}|)$.

In practice, we adapt the proposals in Algorithm 1 to minimize C_{REJ} by using heuristics over the values of $\text{DIST}(\cdot)$ from Proposition 4.

5 Experiments and Results

In this section, we evaluate the Ripple k -node connected induced subgraph (k -CIS) count estimator on several large real world networks. First we show that Ripple outperforms the common baselines in terms of time and space when the pattern sizes are large. Then, we show that our estimator converges when counting both small and large patterns, while varying Ripple’s parameters. Refer to Appendix E for additional results regarding the quality of Ripple Estimator and its parallel implementation.

Execution environment. Our experiments were performed on a dual Intel Xeon Gold 6254 CPU with 72 virtual cores (total) at 3.10GHz, and 392GB of RAM. In addition, this machine is also equipped with a fast SSD NVMe PCIe4 with 800GB of free space available.

Baselines. We use Motivo (Bressan et al., 2019), a fast C++ system for subgraph counting, as the baseline since it is the only method capable of counting large patterns ($k > 6$), to the best of our knowledge. Also, notice that existing *MCMC* methods for subgraph counting like IMPRG (Chen and Lui, 2018) and RGPM (Teixeira et al., 2018) can not count beyond $k = 5$ in practice.

Datasets. In the experiments, we use large networks from SNAP (Leskovec and Krevl, 2014), which represent diverse graph domains and have been used in many other works to evaluate subgraph counting algorithms (Bressan et al., 2018, 2019; Paramonov et al., 2019). Table 1 presents these datasets along with their basic features including the order of magnitude of the subgraph counts $|\mathcal{V}^{(k)}|$ estimated using Ripple for $k \in \{6, 8, 10, 12\}$.

Algorithm 2: Ripple for Subgraph Counting

Input: Input graph G , Order k , Set of subgraph patterns \mathcal{H} of interest
Input: Initial vertex stratum \mathcal{I}_1 , Reservoir Size M and Error Bound ϵ
Output: $\hat{\mu}$, an asymptotically unbiased estimate of $\mathcal{C}^{(k)}$

```

/* Initialization */
1  $\hat{\mu} = 0, \hat{\beta}_{q,t} = 0, \hat{\mathbf{U}}_{q,t} = \emptyset, \forall 1 \leq q < t \leq R;$ 
2 Run BFS for stratification  $\rho: \mathcal{V}^{(k-1)} \rightarrow \{1, \dots, R\}$ , with  $\mathcal{I}_1$  (Proposition 4)

/* Exact computation in the first stratum */
3 foreach  $u \in \mathcal{I}_1, v \in \mathbf{N}_{\mathcal{G}^{(k-1)}}(u)$  do
4   Update  $\hat{\beta}_{1,\rho(v)} += 1, \hat{\mathbf{U}}_{1,\rho(v)} \cup v$ 
5   Update  $\hat{\mu} += \left( \frac{\mathbf{1}_{\{u \circ v \sim H\}}}{\gamma(u \circ v)} \right)_{H \in \mathcal{H}};$  // Equation (10)

/* Estimate remaining strata */
6 for  $r \in 2, \dots, R$  do
7   Initialize  $\hat{\mu}_r = 0, m_r = 0$ 
8   parallel while Equation (12) is not satisfied do
9     Sample  $q$  from  $\{1, \dots, r-1\}$  w.p.  $\hat{\beta}_{q,r}$ 
10    Sample  $u$  from  $\hat{\mathbf{U}}_{q,r};$  // Equation (7)
11    Sample  $v \sim \text{UNIF}(\mathbf{N}_{\mathcal{G}^{(k-1)}}(u));$  // Algorithm 1
12    while  $\rho(v) \geq r$  do
13      Update  $\hat{\mu}_r += \left( \frac{\mathbf{1}_{\{u \circ v \sim H\}}}{\gamma(u \circ v)} \right)_{H \in \mathcal{H}};$  // Equation (9)
14      if  $\rho(v) > r$  then
15        Update  $\hat{\beta}_{r,\rho(v)} += 1;$  // Equation (5)
16        Update  $\hat{\mathbf{U}}_{r,\rho(v)} \cup v;$  // Equation (7)
17       $u := v$ 
18      /* Proposition 2 and Algorithm 1 */
19      if  $\rho(u) = r$  then
20        Sample  $v \sim \text{UNIF}(\mathbf{N}_{\mathcal{G}^{(k-1)}}(u))$ 
21      else
22        while  $\rho(v) \neq r$  do
23          Sample  $v \sim \text{UNIF}(\mathbf{N}_{\mathcal{G}^{(k-1)}}(u))$ 
24       $m_r += 1$ 
25      Compute  $\widehat{\text{deg}}_r = \sum_{q=1}^{r-1} \hat{\beta}_{q,r};$  // Equation (6)
26       $\hat{\mu} += \frac{\widehat{\text{deg}}_r}{2 m_r} \hat{\mu}_r;$  // Equations (8) and (9)
27      Update  $\hat{\beta}_{r,t} *= \frac{\widehat{\text{deg}}_r}{m_r}, \forall t > r;$  // Equation (5)
28 return  $\hat{\mu}$ 

```

Hyper-parameters \mathcal{I}_1 , M and ϵ . As detailed in Section 4, especially 4.5, Ripple provides the aforementioned three hyper-parameters that may be tuned to address the trade off between accuracy and resource consumption. We empirically evaluate this tradeoff for each of these parameters next.

5.1 Scalability Assessment

We start by assessing the scalability of the methods when estimating k -CIS counts for $k \geq 6$. To the best of our knowledge, Motivo is the only existing

Graph	V	E	D_G	Δ_G	Magnitude of Est. # of CISs			
					$ \mathcal{V}^{(6)} $	$ \mathcal{V}^{(8)} $	$ \mathcal{V}^{(10)} $	$ \mathcal{V}^{(12)} $
Amazon	334,863	925,872	44	549	10^{11}	10^{15}	10^{19}	10^{22}
DBLP	317,080	1,049,866	21	343	10^{12}	10^{16}	10^{19}	10^{23}
Cit-Pat.	3,774,768	16,518,948	22	793	10^{14}	10^{18}	10^{22}	10^{26}
Pokec	1,632,803	30,622,564	11	14,854	10^{18}	10^{25}	10^{32}	10^{38}
LiveJ.	3,997,962	34,681,189	17	14,815	10^{19}	10^{25}	10^{32}	10^{38}
Orkut	3,072,441	117,185,083	9	33,313	10^{21}	10^{28}	10^{35}	10^{43}

Table 1: The graph datasets that we used along with some features including the graph diameter D_G , maximum degree of a node in G Δ_G and the orders of magnitude of the estimated number of k -CISs – which increase exponentially – for $k \in \{6, 8, 10, 12\}$.

method capable of estimating such patterns. Each execution of Motivo has two phases: a build-up phase, which constructs an index table in the disk, and a sampling phase that queries this table. In the case of Motivo, we only measure the time taken by the build-up phase and the out-of-core (disk) usage since its bottleneck is the building and merging of treelet tables on disk. As such, we report the best case scenario for Motivo and the reported values are lower bounds for the actual time and space requirement. For Ripple, we estimate the total number of k -CIS and report the total time taken and the maximum resident memory requirement (RAM) as space cost because Ripple works purely in memory.

Tables 3 and 4 compare the running time and space usage, respectively, of Ripple and Motivo. We further measure the rate of increase of these measurements (columns $\text{Time}^{(k)}/\text{Time}^{(k-2)}$ and $\text{Space}^{(k)}/\text{Space}^{(k-2)}$), in terms of the sub-graph size k . We fix the hyper-parameters for Ripple as $\epsilon = 0.003$, $|\mathcal{I}_1| = 10^4$ and $M = 10^7$ based on our analysis in Section 5.2 and Table 2 in Appendix E. For Motivo, we follow the authors’ suggestion and set the number of colors to k (Bressan et al., 2019). To ensure that the space and time measurements are not arbitrary, we report in Table 2 the dispersion of the Ripple estimates computed by the measured runs. The dispersion is defined as the ratio of the range (max - min) of the estimates and the mean.

Running time scalability on k (Table 3). We observe that Motivo often outperforms Ripple for $k = 6, 8$, but it does not scale well for $k = 10, 12$. In the latter case, Motivo requires a significant time to build its indices, which often results in execution termination when available storage space becomes insufficient. Particularly, for DBLP, Motivo took around 10 minutes to process 10-CIS but almost 9 hours for 12-CIS, a growth rate of $58\times$ as reported in the $\text{Time}^{(k)}/\text{Time}^{(k-2)}$ column. On the other hand, not only did Ripple succeed in **all** configurations in less than 4 hours on average, but it also exhibited a smoother growth in running time. The largest increase ratio was $2.7\times$, observed for DBLP and LiveJournal when k went from 8 to 10. Note that $\text{Time}^{(k)}/\text{Time}^{(k-2)} < (k/(k-2))^7$ in all cases according to the time complexity shown in Proposition 6.

Graph	Rel. dispersion of estimates			
	6	8	10	12
Amazon	0.203	0.241	0.285	0.268
DBLP	0.023	0.023	0.041	0.054
Patents	0.037	0.083	0.093	0.123
Pokec	0.065	0.044	0.037	0.046
LiveJ.	0.050	0.060	0.033	0.066
Orkut	0.021	0.761	0.053	0.031

Table 2: (Accuracy of estimates) Dispersion (range/mean) of Ripple’s estimates of $|\mathcal{V}^{(k)}|$ computed using $\epsilon = 0.003$, $|\mathcal{I}_1| = 10^4$ and $M = 10^7$ for each $k \in \{6, 8, 10, 12\}$ and datasets in Table 1. The values reported show that the selected hyper-parameters provide reasonably similar estimates over independent runs. The largest dispersion is observed for $k = 8$ in Orkut due to the presence of a single outlier.

Dataset	k	Motivo Build-up only		Ripple ($\epsilon = 0.003$)		Ripple gains (hrs)
		Time (hrs)	$\frac{\text{Time}^{(k)}}{\text{Time}^{(k-2)}}$	Time (hrs)	$\frac{\text{Time}^{(k)}}{\text{Time}^{(k-2)}}$	
Amazon	6	0.002 ± 0.000	—	0.020 ± 0.000	—	-0.018
	8	0.006 ± 0.000	3×	0.029 ± 0.000	1.4×	-0.023
	10	0.082 ± 0.000	13.7×	0.056 ± 0.000	1.9×	+0.026
	12	3.630 ± 0.002	44.3×	0.095 ± 0.002	1.7×	+3.535
DBLP	6	0.002 ± 0.000	—	0.013 ± 0.000	—	-0.011
	8	0.007 ± 0.000	3.5×	0.030 ± 0.000	2.3×	-0.023
	10	0.156 ± 0.000	22.3×	0.082 ± 0.000	2.7×	+0.074
	12	9.099 ± 0.002	58.3×	0.105 ± 0.002	1.3×	+8.994
Patents	6	0.022 ± 0.000	—	0.033 ± 0.000	—	-0.011
	8	0.098 ± 0.000	4.5×	0.051 ± 0.000	1.5×	+0.047
	10	> 1.1 hrs, crashed	—	0.090 ± 0.001	1.8×	—
	12	> 0.5 hrs, crashed	—	0.117 ± 0.003	1.3×	—
Pokec	6	0.012 ± 0.000	—	0.459 ± 0.142	—	-0.447
	8	0.128 ± 0.000	10.7×	0.759 ± 0.282	1.7×	-0.631
	10	5.965 ± 0.000	46.6×	1.400 ± 0.592	1.8×	+4.565
	12	> 1.5 hrs, crashed	—	1.469 ± 0.334	1×	—
LiveJ.	6	0.024 ± 0.000	—	0.351 ± 0.009	—	-0.327
	8	0.205 ± 0.000	8.5×	0.642 ± 0.074	1.8×	-0.437
	10	> 2.3 hrs, crashed	—	1.76 ± 1.550	2.7×	—
	12	> 0.7 hrs, crashed	—	2.189 ± 1.350	1.2×	—
Orkut	6	0.032 ± 0.000	—	0.669 ± 0.026	—	-0.637
	8	0.585 ± 0.006	18.3×	1.744 ± 0.983	2.6×	-1.159
	10	> 8.9 hrs, crashed	—	2.633 ± 1.065	1.5×	—
	12	> 1.8 hrs, crashed	—	3.967 ± 3.162	1.5×	—

Table 3: Running time comparison between Ripple and Motivo over 6 large networks. As the pattern size increases, Motivo starts to break. The rightmost column shows that Ripple outperforms the baseline on larger values of k , providing gains of up to 9 hours where Motivo is able to complete.

Space scalability on k (Table 4). In terms of the space usage of Motivo compared to Ripple, we see trends similar to the running time analysis above. The rate of increase column (i.e., $\text{Space}^{(k)} / \text{Space}^{(k-2)}$) is very telling of the exponential increase in the space complexity of Motivo w.r.t. k as opposed to the

Dataset	k	Motivo Build-up only		Ripple ($\epsilon = 0.003$)		Ripple gains (GB)
		Space (GB)	$\frac{\text{Space}^{(k)}}{\text{Space}^{(k-2)}}$	Space (GB)	$\frac{\text{Space}^{(k)}}{\text{Space}^{(k-2)}}$	
Amazon	6	0.53 \pm 0.00	—	4.69 \pm 0.06	—	-4.16
	8	4.00 \pm 0.00	7.5 \times	5.73 \pm 0.12	1.2 \times	-1.73
	10	48.00 \pm 0.00	12 \times	7.38 \pm 0.36	1.3 \times	+40.62
	12	559 \pm 0.00	11.6 \times	9.09 \pm 1.02	1.2 \times	+549.91
DBLP	6	0.50 \pm 0.00	—	4.58 \pm 0.02	—	-4.08
	8	4.00 \pm 0.00	8 \times	6.31 \pm 0.00	1.4 \times	-2.31
	10	50.00 \pm 0.00	12.5 \times	7.99 \pm 0.01	1.3 \times	+42.01
	12	611.00 \pm 0.00	12.2 \times	10.45 \pm 0.02	1.3 \times	+600.55
Patents	6	7.00 \pm 0.00	—	11.50 \pm 0.05	—	-4.5
	8	66.00 \pm 0.00	9.4 \times	13.80 \pm 0.03	1.2 \times	+52.2
	10	> 800, <i>crashed</i>	—	15.85 \pm 0.08	1.1 \times	> 800
	12	> 800, <i>crashed</i>	—	18.12 \pm 0.10	1.1 \times	> 800
Pokec	6	3.7 \pm 0.00	—	13.69 \pm 0.06	—	-9.99
	8	36.00 \pm 0.00	9.7 \times	17.17 \pm 0.03	1.3 \times	18.83
	10	407.00 \pm 0.00	11.3 \times	20.31 \pm 0.01	1.2 \times	+386.69
	12	> 800, <i>crashed</i>	—	22.82 \pm 0.03	1.1 \times	> 800
LiveJ.	6	7.70 \pm 0.00	—	18.26 \pm 0.02	—	-10.56
	8	73.00 \pm 0.00	9.5 \times	21.26 \pm 0.00	1.2 \times	+51.74
	10	> 800, <i>crashed</i>	—	24.43 \pm 0.72	1.1 \times	> 800
	12	> 800, <i>crashed</i>	—	27.75 \pm 0.00	1.1 \times	> 800
Orkut	6	7.90 \pm 0.00	—	40.38 \pm 0.00	—	-32.48
	8	78.00 \pm 0.000	9.9 \times	43.49 \pm 0.00	1.1 \times	+34.51
	10	> 800, <i>crashed</i>	—	46.63 \pm 0.00	1.1 \times	> 800
	12	> 800, <i>crashed</i>	—	49.73 \pm 0.00	1.1 \times	> 800

Table 4: Space usage comparison between Ripple and Motivo over 6 large networks. Motivo often runs out of *disk* space in the build-up stage on large datasets for $k \geq 10$, while Ripple keeps its *memory* requirements stable. Ripple uses up to 600 GB less space in cases where Motivo is able to complete.

near-constant increase in Ripple despite its polynomial complexity described in Proposition 6. For Amazon, Motivo’s space demands increase by at least 7.5 \times when k goes from 6 to 8. This overhead is significantly larger when k increases from 10 to 12. For instance, Motivo’s disk usage goes from 50GB to 611GB for DBLP. In larger datasets, Motivo fails to complete for $k = 10, 12$ due to its space complexity. Ripple, on the other hand, shows, overall, only a slight increase w.r.t. space requirement for any k , which may be explained by the cost of maintaining larger subgraphs in the reservoirs. Indeed, the largest rate of increase was 1.4 \times when moving from $k = 6$ to $k = 8$ in DBLP and, moreover, it requires up to 600 GB less space in cases where Motivo was successful.

5.2 Accuracy and Convergence Assessment

Next we evaluate the accuracy and convergence of Ripple on both small and large subgraph patterns. First, we verify the accuracy of our method on counting small k -CIS patterns, i.e., $k \in \{3, 5\}$, where ground truths can be obtained from *ESCAPE* (Pinar et al., 2017). As an accuracy metric, we report the

L2-norm between the estimate and the exact value of the count vector $\mathcal{C}^{(k)}$ (Equation (10)) of all non-isomorphic subgraph patterns of size k . Figure 4 shows results for $k = 5$ (where the number of patterns of interest $|\mathcal{H}| = 21$), for different settings of the parameters ϵ and $|\mathcal{I}_1|$.

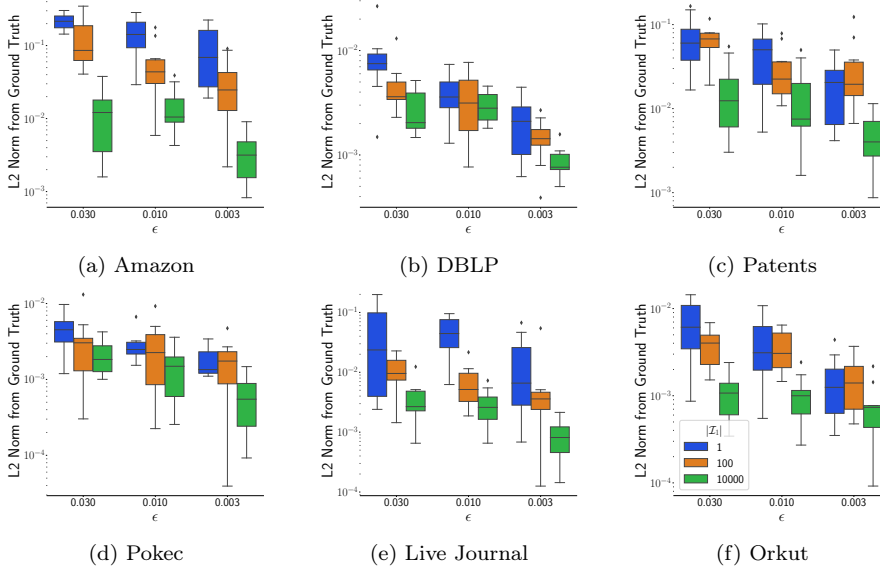


Fig. 4: Accuracy and convergence analysis for 5-CIS s. The y -axes show the L2-norm between the Ripple estimate and the ground truth vector $\mathcal{C}^{(k)}$ (Equation (10)) containing counts of all possible non isomorphic subgraph patterns while varying parameters ϵ and number of subgraphs in \mathcal{I}_1 . As expected, the accuracy improves as ϵ decreases and \mathcal{I}_1 increases. Each box and whisker represents 10 runs.

Accuracy on small k (Figure 4). In all datasets, we note that the L2-norm reduces, on average, as ϵ decreases from 0.3 to 0.003 and as $|\mathcal{I}_1|$ grows from 100 to 10^4 . We realize a reduction close to an order of magnitude between the worst and the best settings, respectively $\epsilon = 0.3$, $|\mathcal{I}_1| = 100$ and $\epsilon = 0.003$, $|\mathcal{I}_1| = 10^4$. This is due to Theorem 2 and Lemma 1 because reducing ϵ leads to a larger number of tours, and consequently lower error in the Ripple estimate. Furthermore, a lower bias in the earlier strata would lead to reduced error propagation. Increasing \mathcal{I}_1 implies in less strata and thus, it also reduces error propagation. Experiment results for $k = 3$ can be found in Appendix E – Figure 8.

Trade-off between convergence and reservoir size (Figure 5). Next we evaluate the trade-off between the reservoir capacity M and accuracy, as discussed in

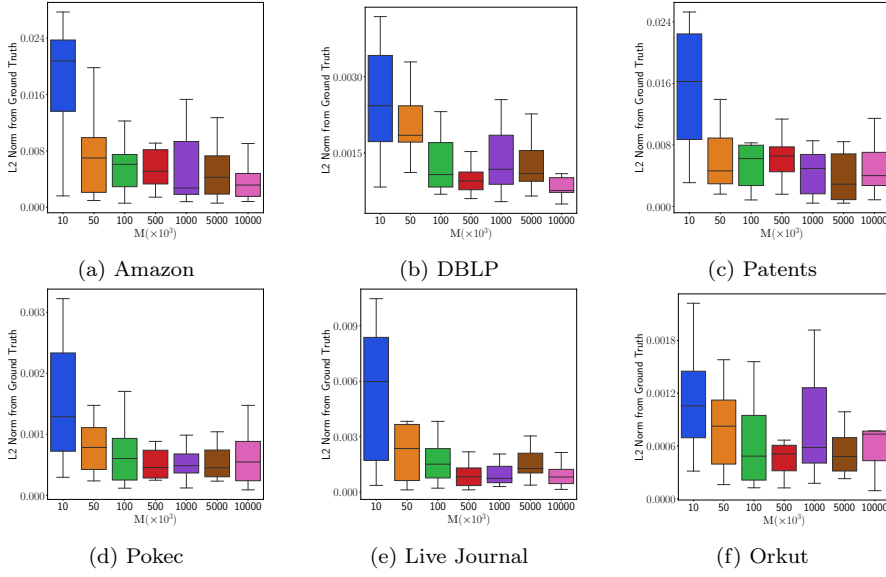


Fig. 5: Sensitivity of Ripple to the reservoir capacity M for $k = 5$. We verify through box and whiskers plots over 10 runs, that a larger reservoir improves the accuracy of Ripple estimates in all graphs since it reduces oversampling bias.

Section 4.3. For that, we vary M from 50000 to 10^7 , while keeping the other parameters fixed as $\epsilon = 0.003$ and $|Z_1| = 10^4$. Like in Section 5.2, we measure the L2-norm among the estimates and the exact value of the subgraph count vectors $\mathcal{C}^{(k)}$ for all non isomorphic subgraph patterns. Figure 5 shows results for $k = 5$, where we see that larger reservoirs reduce oversampling bias and improve both the convergence and accuracy in all datasets. Results for $k = 3$ are deferred to Appendix E – Figure 9.

Convergence for large k (Figure 6). Since computing the ground truth for $k > 5$ is intractable for real world graphs, we show that Ripple converges in these cases, despite higher computing effort. Here we present results for $k = 12$ and defer results for smaller (less challenging) values of k to Appendix E. A reasonable hypothesis is that sparse patterns should be frequent in power-law networks, especially as k grows. We show empirical evidence for such a hypothesis in Figure 6, where we estimate the total number of k -CISs, the number of sparse subgraphs and the number of stars (by choosing an appropriate pattern set \mathcal{H} and equivalence relationship in Definition 11). We define sparse patterns as those subgraphs whose density lies between 0 and 0.25, computed according to Liu and Wong (2008). Indeed, Ripple converges for all datasets and, as expected, most patterns are sparse. The most frequent pattern is by far the star type representing close to half of the patterns in many of the studied networks.

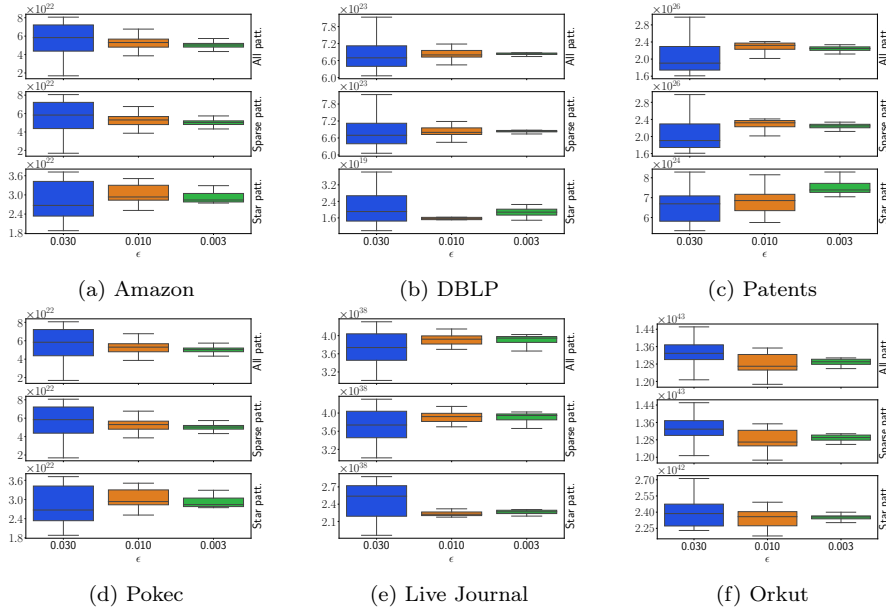


Fig. 6: Convergence of Ripple estimates of 12-*CIS* pattern counts. We estimate the total count of subgraphs $|\mathcal{V}^{(12)}|$, the number of sparse patterns and stars. The estimates over 10 runs are presented as box and whiskers plots which exhibit a reduction in variance as ϵ increases. Indeed, almost all patterns are sparse and the most frequent substructure is a star.

This proportion is attenuated in DBLP and Patents, where dense substructures naturally emerge from collaboration/citation among authors which were used to build these graphs.

6 Related Work

For better presentation, we split this section into two parts where the first deals with parallel *MCMC* techniques and the second deals with methods for subgraph counting.

6.1 Parallel *MCMC* through Splitting

Going as far back as Nummelin (1978); Athreya and Ney (1978), multiple techniques have been proposed to circumvent the uncertainty around the burn in period by splitting the Markov chain into i.i.d. sample paths. This strategy allows the practitioner to compute unbiased estimates in parallel and determine their confidence intervals. Perfect sampling methods that rely on coupling (Propp and Wilson, 1996) and annealing/tempering (Neal, 2001) require

the transition probabilities to satisfy certain conditions. The former example requires the transitions to be monotonic w.r.t. some ordering over the state space and the latter example requires some notion of temperature which are absent in random walks on large diameter graphs. Other coupling based regeneration methods like (Mykland et al., 1995; Jacob et al., 2020; Glynn and Rhee, 2014) require a minorization condition, to hold albeit implicitly.

Regeneration point based methods proposed by Cooper et al. (2016); Massoulié et al. (2006); Avrachenkov et al. (2016, 2018); Savarese et al. (2018); Teixeira et al. (2018) are more general since they don't require any other condition to be satisfied other than standard ergodicity conditions and the chain being finite state. While Cooper et al. (2016) and Massoulié et al. (2006) used random walks tours on simple graphs to estimate its properties, Avrachenkov et al. (2016) proposed the usage of the contracted graph to reduce expected running times. This was further developed in Avrachenkov et al. (2018) using reinforcement learning. Savarese et al. (2018) used supernode-based random walks to estimate partition functions and gradients in *RBM*s, while Teixeira et al. (2018) used *RWT*s to count subgraphs by posing it as a vertex sum problem on the *HON*. To the best of our knowledge, there is no existing work that controls expected running times through stratification.

Unrelated work. Much work has been done to introduce parallelism to efficiently sample transitions where it is intractable or expensive to do so. Notable lines of work include chains involving tall data such as Bardenet et al. (2017) and large graphical models, e.g., Gonzalez et al. (2011). While make each Gibbs sampling step efficient, since the chain is not split, the algorithm still relies on a single long sample path. While Ribeiro and Towsley (2010) provides a way to combine samples from multiple parallel random walks, it still suffers from burn in induced uncertainty.

6.2 Subgraph Counting with Sampling

The combinatorial nature of the subgraph counting problem makes exact solutions often impractical when dealing with large graphs and patterns. This motivated researchers to design scalable sampling methods. Of these, *random walk (RW)* and *color coding (CC)* based algorithms are the two major classes in the literature.

Random walk methods. Many random walk algorithms have been proposed to estimate subgraph pattern *distributions*, which is significantly easier than estimating *counts*. These include GUISE (Bhuiyan et al., 2012b), PSRW (Wang et al., 2014) and more recently, Waddling (Han and Sethu, 2016) and RSS (Matsumoto and Gionis, 2020). While the first uses a Metropolis-Hastings (Hastings, 1970) algorithm to sample subgraphs uniformly, PSRW uses a random walk over the higher order networks. Waddling performs a simple random walk over the original graph and uses the last visited nodes to sample subgraphs and RSS

applies Metropolis-Hastings and canonical paths (Sinclair, 1992) to improve the mixing time of the underlying Markov Chain. For subgraph counting, Chen and Lui (2018) proposed IMPRG, which uses a random walk method similar to Waddling, but employ specific estimators designed for up to 5-node patterns. IMPRG requires computing Hamiltonian paths on k -node subgraphs making it hard to scale on large patterns. While RGPM uses *RWTs* to compute unbiased estimates of subgraph counts, the method is tractable only for $k \leq 5$ due to the spectral gap of higher order networks (please, check (Bressan et al., 2018; Matsuno and Gionis, 2020)). In summary, existing random walk methods, although memory-efficient, are unable to estimate pattern counts beyond $k > 5$ in practice.

Color-coding based methods. Motivo (Bressan et al., 2019) is an example of such methods where the key step is to build an index table using a deterministic dynamic programming algorithm, which is then exploited to sample subgraphs uniformly and i.i.d. The *CC*-based approach was first proposed to count tree-like patterns (and variants) (Alon et al., 2008; Zhao et al., 2010; Slota and Madduri, 2014; Chakaravarthy et al., 2016) and was extended by Bressan et al. (2018) by accounting for the number of spanning trees associated with each subgraph to estimate subgraph counts. However, *CC* methods suffer from the exponential time and space complexities associated with building and accessing the index table. Motivo improved these algorithms by proposing succinct index tables and efficient out-of-core I/O mechanisms to ameliorate this issue. This extended the applicability of *CC* methods for larger subgraphs.

Other methods. The Mfinder method (Kashtan et al., 2004), a pioneer in motif estimation, introduced neighborhood sampling where starting with a random vertex, a k node subgraph is sampled by recruiting neighbors of already recruited vertices; samples so generated are then used estimate counts of the subgraph. Wernicke (2006) proposed FANMOD, a method that receives an additional parameter (besides subgraph size): the *fraction* of subgraphs that should be sampled from the whole search space. Based on this fraction, the subgraph extension is rearranged in a way that every k -subgraph is sampled uniformly at random. For large subgraph pattern, however, FANMOD may be impractical leading to a huge number of rejections. ASAP (Iyer et al., 2018), SSRW (Yang et al., 2018) and Lift (Paramonov et al., 2019) use a similar neighborhood expansion strategy, although the former is distributed. Lift can estimate subgraph counts, but computing the sampling probability requires an iteration over all possible sample paths that may generate a subgraph which is $O(k!)$ and limit their results to $k \leq 6$. SSRW presents the same limitation that Lift, but they showed results for up to $k = 7$. MOSS (Wang et al., 2018) uses a variant of the Mfinder approach to rapidly estimates 5-node subgraph counts by deriving estimates of some 5-node subgraphs types from other ones. Other methods to sample subgraphs have also been proposed by Jain and Seshadhri (2017, 2020) and Liu et al. (2020). The first exploits the Turán’s Theorem for subgraph counting, but it estimates near-clique patterns only. In the second,

authors learned models to predict the subgraph isomorphism counts through deep graph representation learning. Here they assume a pattern template as reference, differently from general subgraph counting. Please, check Ribeiro et al. (2019) for a survey.

7 Conclusions

In this paper we propose the Ripple estimator that uses *sequentially stratified regenerations* to control the running time of random walk tour based *MCMC*. We prove that the Ripple estimator is consistent (w.r.t. the number of random walk tours), and that the time and memory complexity of our implementation for the subgraph counting problem is linear in the number of patterns of interest and polynomial in the subgraph size. We empirically verified our claims on multiple graph datasets and showed that Ripple can accurately estimate subgraph pattern counts with a smaller memory footprint, compared to the state-of-the-art, Motivo (Bressan et al., 2019). Ripple is currently the only subgraph pattern count estimator that is able to estimate $k = 10, 12$ node patterns in million-node graphs. Beyond our specific application, Ripple provides a promising way to expand the sphere of influence of regenerative simulation in discrete reversible *MCMC*.

References

- Aldous D, Fill JA (2002) Reversible markov chains and random walks on graphs. Unfinished monograph, recompiled 2014, available at <http://www.stat.berkeley.edu/~aldous/RWG/book.html>
- Alon N, Dao P, Hajirasouliha I, Hormozdiari F, Sahinalp SC (2008) Biomolecular network motif counting and discovery by color coding. *Bioinformatics* 24(13):i241–i249
- Athreya KB, Ney P (1978) A new approach to the limit theory of recurrent markov chains. *Transactions of the American Mathematical Society* 245:493–501
- Avrachenkov K, Ribeiro B, Sreedharan JK (2016) Inference in osns via lightweight partial crawls. In: *ACM SIGMETRICS*, pp 165–177
- Avrachenkov K, Borkar VS, Kadavankandy A, Sreedharan JK (2018) Revisiting random walk based sampling in networks: evasion of burn-in period and frequent regenerations. *Computational social networks* 5(1):1–19
- Bardenet R, Doucet A, Holmes C (2017) On markov chain monte carlo methods for tall data. *The Journal of Machine Learning Research* 18(1):1515–1557
- Bhuiyan MA, Rahman M, Rahman M, Al Hasan M (2012a) Guise: Uniform sampling of graphlets for large graph analysis. In: *Proceedings of the 2012 IEEE 12th International Conference on Data Mining*

- Bhuiyan MA, Rahman M, Rahman M, Al Hasan M (2012b) Guise: Uniform sampling of graphlets for large graph analysis. In: 2012 IEEE 12th International Conference on Data Mining, IEEE, pp 91–100
- Bremaud P (2001) Markov Chains: Gibbs Fields, Monte Carlo Simulation, and Queues. Texts in Applied Mathematics, Springer New York
- Bressan M, Chierichetti F, Kumar R, Leucci S, Panconesi A (2018) Motif counting beyond five nodes. ACM TKDD 12(4)
- Bressan M, Leucci S, Panconesi A (2019) Motivo: Fast motif counting via succinct color coding and adaptive sampling. Proc VLDB Endow 12(11):1651–1663, DOI 10.14778/3342263.3342640, URL <https://doi.org/10.14778/3342263.3342640>
- Chakaravarthy VT, Kapralov M, Murali P, Petrini F, Que X, Sabharwal Y, Schieber B (2016) Subgraph counting: Color coding beyond trees. In: 2016 IEEE International Parallel and Distributed Processing Symposium (IPDPS), Ieee, pp 2–11
- Chen X, Lui JC (2018) Mining graphlet counts in online social networks. ACM TKDD 12(4):1–38
- Chung FR, Graham FC (1997) Spectral graph theory. 92, American Mathematical Soc.
- Cooper C, Radzik T, Siantos Y (2016) Fast low-cost estimation of network properties using random walks. Internet Mathematics
- Diaconis P, Stroock D (1991) Geometric bounds for eigenvalues of markov chains. The Annals of Applied Probability pp 36–61
- Geman S, Geman D (1984) Stochastic relaxation, gibbs distributions, and the bayesian restoration of images. IEEE Transactions on pattern analysis and machine intelligence (6):721–741
- Geyer CJ (1992) Practical markov chain monte carlo. Statistical science pp 473–483
- Glynn PW, Rhee Ch (2014) Exact estimation for markov chain equilibrium expectations. Journal of Applied Probability 51(A):377–389
- Gonzalez J, Low Y, Gretton A, Guestrin C (2011) Parallel gibbs sampling: From colored fields to thin junction trees. In: Proceedings of the Fourteenth International Conference on Artificial Intelligence and Statistics, pp 324–332
- Han G, Sethu H (2016) Waddling random walk: Fast and accurate mining of motif statistics in large graphs. In: ICDM, IEEE, pp 181–190
- Hastings WK (1970) In: Monte Carlo sampling methods using Markov chains and their applications, Oxford University Press
- Hopcroft J, Tarjan R (1973) Algorithm 447: efficient algorithms for graph manipulation. Communications of the ACM 16(6):372–378
- Iyer AP, Liu Z, Jin X, Venkataraman S, Braverman V, Stoica I (2018) {ASAP}: Fast, approximate graph pattern mining at scale. In: OSDI, pp 745–761
- Jacob PE, O’Leary J, Atchadé YF (2020) Unbiased markov chain monte carlo methods with couplings. Journal of the Royal Statistical Society: Series B (Statistical Methodology) 82(3):543–600
- Jain S, Seshadhri C (2017) A fast and provable method for estimating clique counts using turán’s theorem. In: Proceedings of the 26th International Con-

- ference on World Wide Web, WWW '17, pp 441–449
- Jain S, Seshadhri C (2020) Provably and efficiently approximating near-cliques using the turán shadow: Peanuts. In: Proceedings of The Web Conference 2020, pp 1966–1976
- Kashtan N, Itzkovitz S, Milo R, Alon U (2004) Efficient sampling algorithm for estimating subgraph concentrations and detecting network motifs. *Bioinformatics* 20(11):1746–1758
- Leskovec J, Krevl A (2014) SNAP Datasets: Stanford large network dataset collection. <http://snap.stanford.edu/data>
- Liu G, Wong L (2008) Effective pruning techniques for mining quasi-cliques. In: ECML-PKDD
- Liu X, Pan H, He M, Song Y, Jiang X, Shang L (2020) Neural subgraph isomorphism counting. In: Proceedings of the 26th ACM SIGKDD International Conference on Knowledge Discovery & Data Mining, pp 1959–1969
- Massoulié L, Le Merrer E, Kermarrec AM, Ganesh A (2006) Peer counting and sampling in overlay networks: random walk methods. In: Proceedings of the twenty-fifth annual ACM symposium on Principles of distributed computing, pp 123–132
- Matsuno R, Gionis A (2020) Improved mixing time for k-subgraph sampling. In: Proceedings of the 2020 SIAM International Conference on Data Mining, SIAM, pp 568–576
- Mykland P, Tierney L, Yu B (1995) Regeneration in markov chain samplers. *Journal of the American Statistical Association* 90(429):233–241
- Neal RM (2001) Annealed importance sampling. *Statistics and computing* 11(2):125–139
- Neiswanger W, Wang C, Xing E (2014) Asymptotically exact, embarrassingly parallel mcmc. Proceedings of the Thirtieth Conference on Uncertainty in Artificial Intelligence
- Nummelin E (1978) A splitting technique for harris recurrent markov chains. *magazine for "u r probability theory and related areas* 43(4):309–318
- Paramonov K, Shemetov D, Sharpnack J (2019) Estimating graphlet statistics via lifting. In: SIGKDD, p 587–595
- Pinar A, Seshadhri C, Vishal V (2017) Escape: Efficiently counting all 5-vertex subgraphs. In: Proceedings of the 26th International Conference on World Wide Web, pp 1431–1440
- Propp JG, Wilson DB (1996) Exact sampling with coupled markov chains and applications to statistical mechanics. *Random Structures & Algorithms* 9(1-2):223–252
- Ribeiro B, Towsley D (2010) Estimating and sampling graphs with multi-dimensional random walks. In: Proceedings of the 10th ACM SIGCOMM conference on Internet measurement, pp 390–403
- Ribeiro B, Towsley D (2012) On the estimation accuracy of degree distributions from graph sampling. In: CDC
- Ribeiro P, Paredes P, Silva ME, Aparicio D, Silva F (2019) A survey on subgraph counting: Concepts, algorithms and applications to network motifs and graphlets. arXiv preprint arXiv:191013011

- Robert C, Casella G (2013) Monte Carlo statistical methods. Springer Science & Business Media
- Rosenthal JS (1995) Minorization conditions and convergence rates for markov chain monte carlo. *Journal of the American Statistical Association* 90(430):558–566
- Savarese PH, Kakodkar M, Ribeiro B (2018) From monte carlo to las vegas: Improving restricted boltzmann machine training through stopping sets. In: *AAAI*
- Sinclair A (1992) Improved bounds for mixing rates of markov chains and multicommodity flow. *Combinatorics, probability and Computing* 1(4):351–370
- Slota GM, Madduri K (2014) Complex network analysis using parallel approximate motif counting. In: *2014 IEEE 28th International Parallel and Distributed Processing Symposium, IEEE*, pp 405–414
- Teixeira CH, Cotta L, Ribeiro B, Meira W (2018) Graph pattern mining and learning through user-defined relations. In: *ICDM, IEEE*, pp 1266–1271
- Vitter JS (1985) Random sampling with a reservoir. *ACM Transactions on Mathematical Software (TOMS)*
- Wang P, Lui JCS, Ribeiro B, Towsley D, Zhao J, Guan X (2014) Efficiently estimating motif statistics of large networks. *ACM TKDD* 9(2)
- Wang P, Zhao J, Zhang X, Li Z, Cheng J, Lui JCS, Towsley D, Tao J, Guan X (2018) Moss-5: A fast method of approximating counts of 5-node graphlets in large graphs. *IEEE TKDE*
- Wernicke S (2006) Efficient detection of network motifs. *IEEE/ACM Trans Comput Biol Bioinformatics*
- Wilkinson DJ (2006) Parallel bayesian computation. *Statistics Textbooks and Monographs* 184:477
- Yang C, Lyu M, Li Y, Zhao Q, Xu Y (2018) Ssrw: a scalable algorithm for estimating graphlet statistics based on random walk. In: *International Conference on Database Systems for Advanced Applications, Springer*, pp 272–288
- Yao P, Zheng L, Zeng Z, Huang Y, Gui C, Liao X, Jin H, Xue J (2020) A locality-aware energy-efficient accelerator for graph mining applications. In: *2020 53rd Annual IEEE/ACM International Symposium on Microarchitecture (MICRO)*, pp 895–907, DOI 10.1109/MICRO50266.2020.00077
- Zhao Z, Khan M, Kumar VA, Marathe MV (2010) Subgraph enumeration in large social contact networks using parallel color coding and streaming. In: *ICPP, IEEE*, pp 594–603

A Additional Comments

A.1 Generality of the Edge Sum Task

We focus on the simple random walk from Definition 1 as a solution to the edge sum task (Equation (1)) because Markov chains used in most discrete reversible *MCMC* settings can be shown to be equivalent to a random walk on a simple graph as follows.

Remark 4 (Φ - \mathcal{G} equivalence (Diaconis and Stroock, 1991)) Given a time homogenous Markov chain Φ on finite state space \mathcal{V} with transition probability p_Φ reversible relative to stationary distribution π_Φ . A random walk on the weighted undirected graph $\mathcal{G} = (\mathcal{V}, \mathcal{E})$ is governed by Φ when the edge weight function Q is derived from the detailed balance test,

$$Q(u, v) = \pi_\Phi(u) p_\Phi(u, v) = \pi_\Phi(v) p_\Phi(v, u), \quad u, v \in \mathcal{V},$$

such that $(u, v) \in \mathcal{E}$ if $Q(u, v) > 0$.

Secondly we focus on edge sums rather than vertex sums because the ability to do the former implies the latter. As such Proposition 7 generalizes to most discrete, reversible MCMC objectives. Another subtle observation is that the stationary distribution of Φ over the edges is the importance sampling distribution that minimizes the variance of an edge sum estimate (Robert and Casella, 2013), a fact that doesn't hold for vertex sums.

A.2 MCMC Estimates

When the volume (number of edges $|\mathcal{E}|$) of \mathcal{G} is unknown, the MCMC (Geyer, 1992; Geman and Geman, 1984; Hastings, 1970) estimate of $\mu^{(\mathcal{E})}/|\mathcal{E}|$ is given by:

Proposition 7 (MCMC Estimate) *When the graph \mathcal{G} from Definition 1 is connected, the random walk Φ is reversible and positive recurrent with stationary distribution $\pi_\Phi(u) = \mathbf{d}(u)/\text{Vol}(\mathcal{G})$, where $\text{Vol}(\mathcal{G})$ is the volume of \mathcal{G} . As such, the MCMC estimate*

$$\hat{\mu}_0((X_i)_{i=1}^t) = \frac{1}{t-1} \sum_{i=1}^{t-1} f(X_i, X_{i+1}),$$

computed using an arbitrarily started sample path $(X_i)_{i=1}^t$ from Φ is an asymptotically unbiased estimate of $\mu^{(\mathcal{E})}/|\mathcal{E}|$. When \mathcal{G} is non bipartite, i.e. Φ is aperiodic, and t is large, $\hat{\mu}_0$ converges to $\mu^{(\mathcal{E})}/|\mathcal{E}|$ as

$$\left| \mathbb{E}[\hat{\mu}_0((X_i)_{i=1}^t)] - \mu^{(\mathcal{E})}/|\mathcal{E}| \right| \leq B \frac{C}{t\delta(\Phi)},$$

where $\delta(\Phi)$ is the spectral gap of Φ and $C \triangleq \sqrt{\frac{1 - \pi_\Phi(X_1)}{\pi_\Phi(X_1)}}$ such that $f(\cdot) \leq B$.

Proof (Proof of asymptotic unbiasedness) Since \mathcal{G} is undirected, finite and connected, Φ is a finite state space, irreducible, time homogeneous Markov Chain and is therefore positive recurrent (Bremaud, 2001, 3-Thm.3.3). The reversibility and stationary distribution holds from the detailed balance test (Bremaud, 2001, 2-Cor.6.1) since

$$\pi_\Phi(u) p_\Phi(u, v) = \pi_\Phi(v) p_\Phi(v, u) = \frac{\mathbf{1}\{(u, v) \in \mathcal{E}\}}{\text{Vol}(\mathcal{G})}.$$

The Ergodic theorem (Bremaud, 2001, 3-Cor.4.1) then applies since f is bounded and we have

$$\lim_{t \rightarrow \infty} \frac{1}{t-1} \sum_{i=1}^{t-1} f(X_i, X_{i+1}) = \sum_{(u,v) \in \mathcal{V} \times \mathcal{V}} \pi_\Phi(u) p_\Phi(u, v) f(u, v) = \frac{\mu(\mathcal{E})}{|\mathcal{E}|},$$

completing the proof. \square

Proof (Proof of bias) Let the i -step transition probability of Φ be given by $p_\Phi^i(u, v)$. The bias at the i -th step is given by

$$\begin{aligned} \text{BIAS}_i &= \left| \mathbb{E}[f(X_i, X_{i+1})] - \sum_{(u,v) \in \mathcal{V} \times \mathcal{V}} \pi_\Phi(u) p_\Phi(u, v) f(u, v) \right| \\ &= \left| \sum_{(u,v) \in \mathcal{V} \times \mathcal{V}} p_\Phi^i(X_1, u) p_\Phi(u, v) f(u, v) - \sum_{(u,v) \in \mathcal{V} \times \mathcal{V}} \pi_\Phi(u) p_\Phi(u, v) f(u, v) \right| \\ &\leq B \left| \sum_{u \in \mathcal{V}} p_\Phi^i(X_1, u) \sum_{v \in \mathcal{V}} p_\Phi(u, v) - \sum_{u \in \mathcal{V}} \pi_\Phi(u) \sum_{v \in \mathcal{V}} p_\Phi(u, v) \right| \\ &\leq B \left| \sum_{u \in \mathcal{V}} p_\Phi^i(X_1, u) - \sum_{u \in \mathcal{V}} \pi_\Phi(u) \right| \leq B \sum_{u \in \mathcal{V}} |p_\Phi^i(X_1, u) - \pi_\Phi(u)|, \end{aligned}$$

where $f(\cdot) \leq B$ and the final inequality is due to Jensen's inequality. From (Diaconis and Stroock, 1991, Prop-3),

$$\text{BIAS}_i \leq B \sqrt{\frac{1 - \pi_\Phi(X_1)}{\pi_\Phi(X_1)}} \beta_*^i,$$

where $\beta_* = 1 - \delta(\Phi)$ is the SLEM of Φ . Since

$$\left| \mathbb{E}[\hat{\mu}_0((X_i)_{i=1}^t)] - \frac{\mu(\mathcal{E})}{|\mathcal{E}|} \right| \leq \frac{1}{t-1} \sum_{i=1}^{t-1} \text{BIAS}_i,$$

due to Jensen's inequality, by using the standard formula for the sum of a GP, we have

$$\left| \mathbb{E}[\hat{\mu}_0((X_i)_{i=1}^t)] - \frac{\mu(\mathcal{E})}{|\mathcal{E}|} \right| \leq \frac{B}{t-1} \sqrt{\frac{1 - \pi_\Phi(X_1)}{\pi_\Phi(X_1)}} \frac{1 - \beta_*^t}{1 - \beta_*}.$$

Assuming that $\beta_*^t \approx 0$ and $t-1 \approx t$, when t is large enough completes the proof. \square

A.3 Formal Justification for Ignoring Self Loops

Lemma 2 *Given a contracted graph \mathcal{G}_I from Definition 1 with supernode ζ_I , and the bounded function f from Equation (1) let $h(u, v) \triangleq \mathbf{1}\{u, v \notin I\} \times f(u, v)$, where $\mathbf{1}\{\cdot\}$ is the indicator. Let Φ_I be the random walk on \mathcal{G}_I and let Φ'_I be a chain with transition probabilities equivalent to Φ_I except that it ignores self loops on ζ_I . Then $\mathbb{E}_{\Phi'_I}[\hat{\mu}_*(\mathbf{X}; h)] = \mathbb{E}_{\Phi_I}[\hat{\mu}_*(\mathbf{X}; h)] = \mu(\mathcal{E} \setminus \mathcal{E}_*)$, where $\hat{\mu}_*$ is defined in Equation (2) from Lemma 1 and \mathbf{X} is an RWT sampled on the appropriate chain from ζ_I . Moreover*

$$\text{Var}_{\Phi'_I}(\hat{\mu}_*(\mathbf{X}; h)) \leq \text{Var}_{\Phi_I}(\hat{\mu}_*(\mathbf{X}; h)).$$

Proof Let \mathcal{X} be the set of all tours from ζ with positive measure according to Φ_I defined later in Lemma 4 within Appendix C.5. Let $F: \mathcal{X} \rightarrow \mathbb{R}$ be defined as $F(\mathbf{X}) = \sum_{j=1}^{|\mathbf{X}|} h(X_j, X_{j+1}) = \sum_{j=2}^{|\mathbf{X}|} f(X_j, X_{j+1})$, where the second equality is by the definition of h . Further note that $\sum_{(u,v) \in \mathcal{E}_I} h(u, v) = \sum_{(u,v) \in \mathcal{E}'_I} h(u, v) = \mu(\mathcal{E} \setminus \mathcal{E}_*)$

Now since the chains are only different at ζ where the $\text{supp}(p_{\Phi'_I}(\zeta, \cdot)) \subseteq \text{supp}(p_{\Phi_I}(\zeta, \cdot))$ Lemma 4 defined later in Appendix C.5 directly applies here and we have

$$\mathbb{E}_{\Phi_I} \left[\frac{p_{\Phi'_I}(\zeta, X_2)}{p_{\Phi_I}(\zeta, X_2)} F(\mathbf{X}) \right] = \mathbb{E}_{\Phi_I} \left[\frac{d_{\mathcal{G}_I}(\zeta)}{d_{\mathcal{G}'_I}(\zeta)} F(\mathbf{X}) \right] = \mathbb{E}_{\Phi'_I} [F(\mathbf{X})],$$

therefore

$$\mathbb{E}_\Phi [\mathbf{d}(\zeta) F(\mathbf{X})] = \mathbb{E}_{\Phi'} [\mathbf{d}'(\zeta) F(\mathbf{X})].$$

Note that $\mathbf{d}_{\mathcal{G}_I}(\zeta)F(\mathbf{X}) = \hat{\mu}_*(\mathbf{X}; h, \mathcal{G}_I)$ and $\mathbf{d}_{\mathcal{G}'_I}(\zeta)F(\mathbf{X}) = \hat{\mu}_*(\mathbf{X}; h, \mathcal{G}'_I)$.

Therefore $\mathbb{E}[\hat{\mu}_*(\mathbf{X}; h, \mathcal{G}_I)] = \mathbb{E}[\hat{\mu}_*(\mathbf{X}; h, \mathcal{G}'_I)] = \mu(\mathcal{E} \setminus \mathcal{E}_*)$

Next, defining the function $F'(\mathbf{X}) = F(\mathbf{X})^2$ with domain \mathcal{X} and applying Lemma 4 yields

$$\mathbb{E}_{\Phi} [\mathbf{d}(\zeta)F(\mathbf{X})^2] = \mathbb{E}_{\hat{\Phi}} [\mathbf{d}'(\zeta)F(\mathbf{X})^2] ,$$

and since $\mathbf{d}(\zeta) \geq \mathbf{d}'(\zeta)$

$$\mathbb{E}_{\Phi} [\mathbf{d}(\zeta)^2 F(\mathbf{X})^2] \geq \mathbb{E}_{\hat{\Phi}} [\mathbf{d}'(\zeta)^2 F(\mathbf{X})^2] ,$$

therefore

$$\mathbb{E}_{\Phi} [\hat{\mu}_*(\mathbf{X}; h, \mathcal{G}_I)^2] \geq \mathbb{E}_{\hat{\Phi}} [\hat{\mu}_*(\mathbf{X}; h, \mathcal{G}_I)^2] ,$$

since the first moments are equal, the variance will depend only on the second moments. Thus $\text{Var}(\hat{\mu}_*(\mathbf{X}; h, \mathcal{G}'_I)) \leq \text{Var}(\hat{\mu}_*(\mathbf{X}; h, \mathcal{G}_I))$ \square

As such for the task of estimating the edge sum over edges not incident on the supernode $\mu(\mathcal{E} \setminus \mathcal{E}_*)$, ignoring self loops reduces the variance of the *RWT* Estimate.

A.4 Articulation Points

Apart from using articulation points in the rejection sampling algorithm from Algorithm 1, we also use them to efficiently compute the subgraph bias γ from Equation (10).

Remark 5 Recall $\gamma(\cdot)$ from Equation (10) which is to be evaluated on every edge sampled by the random walk. Given the $k-1$ -*CIS*, s , $\gamma(s) = \binom{\kappa - \mathcal{A}_s}{2}$, where \mathcal{A}_s is the set of articulation points of s .

The above statement draws directly from (Wang et al., 2014, Sec-3.3) and the definition of articulation points.

Hopcroft and Tarjan (1973) showed that for any simple graph s , given its DFS-tree, a vertex $u \in V(s)$ is an articulation point if any of the following conditions hold.

- a) u is the root node with two or more subtrees.
- b) u is an internal node (non leaf) such that no descendant of u shares an edge with an ancestor of u .

This is illustrated in Figure 7 for a 7-*CIS* with 3 articulation points. Hopcroft and Tarjan (1973) also proposed an $O(|V(s)| + |E(s)|)$ algorithm to check the above conditions while constructing the DFS tree which we reproduce in Algorithm 3.

In Algorithm 3, $\text{LEVEL}[v]$ keeps the level of the node v in the DFS-tree, while $\text{LOW}[v]$ contains the lowest level accessible by some descendent of v . During the search, we may visit some node twice. For example, in Figure 7, v_1 can be reached from v_5 despite being the root. In this case, $\text{LOW}[v_5]$ needs to be updated (Line 14). Any node v is an articulation point iff at least one of its descendants has a higher Low value than v (Lines 11 and 12).

B Proofs for Section 2

B.1 Proof of Lemma 1

Lemma 3 (Avrachenkov et al. (2016)) *Let Φ be a finite state space, irreducible, time homogeneous Markov Chain and let ξ denote the return time of RWT started from some $x_0 \in \mathcal{S}$ as defined in Definition 2. If Φ is reversible then*

$$\mathbb{E} [\xi^2] \leq \frac{3}{\pi_{\Phi}(x_0)^2 \delta(\Phi)} , \quad (13)$$

where $\pi_{\Phi}(x_0)$ is the stationary distribution of x_0 and $\delta(\Phi)$ is the spectral gap of Φ . When Φ is not reversible the second moment of return times is given by Equation (14).

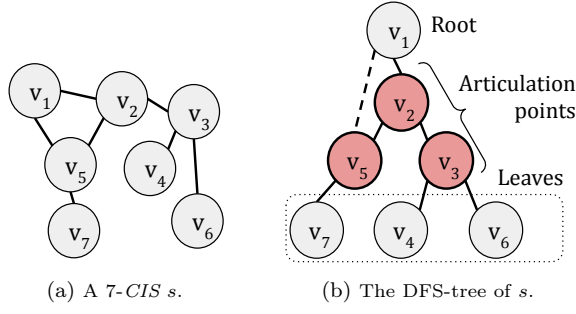


Fig. 7: Articulation points: Figure 7a shows an example of a 7-CIS s whose DFS-tree is shown in Figure 7b. Hopcroft and Tarjan (1973) used such a tree to identify articulation points, i.e. vertices whose removal disconnects the graph, efficiently in $O(|V(s)| + |E(s)|)$ as detailed in Algorithm 3. Note how removing either v_2 , v_3 , or v_5 disconnects s .

Algorithm 3: Articulation Points

Input: Simple Graph $G = (V, E)$
Output: Articulation Points \mathcal{A}_G
 /* Initialization */
 1 $l = 0$;
 2 $\text{LEVEL}[v] = -1, \forall v \in V$;
 3 $\mathcal{A}_G = \emptyset$;
 4 **Function** DFS-AP(v):
 5 $\text{LEVEL}[v] = l + 1$;
 6 $\text{LOW}[v] = \text{LEVEL}[v]$;
 7 **foreach** $u \in N(v)$ **do**
 8 **if** $\text{LEVEL}[u] = -1$ **then**
 9 DFS-AP(u);
 10 $\text{LOW}[v] = \min(\text{LOW}[v], \text{LOW}[u])$;
 11 **if** $\text{LOW}[u] \geq \text{LEVEL}[v]$ **then**
 12 $\mathcal{A}_G = \mathcal{A}_G \cup \{v\}$;
 13 **else if** u is not parent of v **then**
 14 $\text{LOW}[v] = \min(\text{LOW}[v], \text{LEVEL}[u])$;
 15 **End Function**
 16 **foreach** $v \in V$ **do**
 17 DFS-AP(v);
 18 **return** \mathcal{A}_G

Proof Using (Aldous and Fill, 2002, Eq 2.21) we have

$$\mathbb{E}[\xi^2] = \frac{1 + 2\mathbb{E}_{\pi_{\Phi}}(T_{x_0})}{\pi_{\Phi}(x_0)}, \quad (14)$$

where $\mathbb{E}_{\pi_{\Phi}}(T_{x_0})$ is the expected hitting time of x_0 for a Markov chain starting in steady state. Combining (Aldous and Fill, 2002, Lemma 2.11 and Eq 3.41), accounting for continuization and some algebra yields

$$\mathbb{E}_{\pi_{\Phi}}(T_{x_0}) \leq \frac{1}{\pi_{\Phi}(x_0)\delta(\Phi)}. \quad (15)$$

Therefore

$$\mathbb{E}[\xi^2] \leq \frac{1 + \frac{2}{\pi_{\Phi}(x_0)\delta(\Phi)}}{\pi_{\Phi}(x_0)} < \frac{3}{\pi_{\Phi}(x_0)^2\delta(\Phi)}, \quad (16)$$

since both $\pi_{\Phi}(x_0)$ and $\delta(\Phi)$ lie in the interval $(0, 1)$. \square

Proposition 8 *Given a positive recurrent Markov chain Φ over state space \mathcal{S} and a set of m RWTs \mathcal{T} , when the tours are stitched together as defined next, the sample path is governed by Φ . For $t \geq 1$, define*

$$\Phi_t = X_{t-R_{N_t}}^{N_t}$$

where $R_i = \sum_{i'=1}^{i-1} |\mathbf{X}^{i'}|$ when $i > 1$ and $R_1 = 0$ and $N_t = \max i: R_i < t$ and an arbitrary ordering is assumed over \mathcal{T} with $\mathbf{X}^{(i)}$ being the i th RWT in \mathcal{T} . $\mathbf{X}^{(i)}$ and $|\mathbf{X}^{(i)}|$ are both i.i.d. processes such that $\mathbb{E}[|\mathbf{X}^{(i)}|] < \infty$.

Proof Note that R_i is a sequence of stopping times and as such the Strong Markov Property (Bremaud, 2001, 2-Thm.7.1) states that sample paths before and after R_i are independent and are both governed by Φ . Further since Φ is positive recurrent and x_0 is visited i.o. the Regenerative Cycle Theorem (Bremaud, 2001, 2-Thm.7.4) also applies which states that these trajectories are identically distributed. As such these trajectories can be sampled independently as described in the definition of the RWT in Definition 2. $\mathbb{E}[|\mathbf{X}^{(i)}|] < \infty$ due to positive recurrence. \square

Since \mathcal{G} is connected, Proposition 7 implies that Φ is positive recurrent and has steady state given by $\pi_{\Phi}(u) \propto \mathbf{d}(u)$.

Proof (Proof of Unbiasedness and Consistency) Define the reward process for all $i \geq 1$, as $F^{(i)} = \sum_{j=1}^{|\mathbf{X}^{(i)}|} f(X_j^{(i)}, X_{j+1}^{(i)})$, where $\mathbf{X}^{(i)}$ is the i th RWT in \mathcal{T} . Since \mathcal{G} is connected Proposition 8 applies and $F^{(i)}$ and $|\mathbf{X}^{(i)}|$ are both i.i.d sequences. Since $F^{(i)} \leq B|\mathbf{X}^{(i)}|$, both the above sequences have finite first moments. Let N_t and R_i be as defined in Proposition 8.

Therefore from the Renewal Reward Theorem (Bremaud, 2001, 3-Thm.4.2) we have

$$\frac{\mathbb{E}[F^{(i)}]}{\mathbb{E}[|\mathbf{X}^{(i)}|]} = \lim_{t \rightarrow \infty} \frac{\sum_{i=1}^{N_t} F^{(i)}}{t} = \lim_{t \rightarrow \infty} \frac{\sum_{i=1}^{N_t} F^{(i)}}{R_{N_t}} \cdot \frac{R_{N_t}}{t} = \frac{\sum_{i=1}^{N_t} F^{(i)}}{R_{N_t}},$$

where the final equality is because $\lim_{t \rightarrow \infty} \frac{R_{N_t}}{t} = 1 - \lim_{t \rightarrow \infty} \frac{t-R_{N_t}}{t}$ and $\lim_{t \rightarrow \infty} \frac{t-R_{N_t}}{t}$ converges to 0 as $t \rightarrow \infty$ since Φ is positive recurrent implying that with probability 1 tour lengths are $< \infty$.

Note from Proposition 8 and the definition of $F^{(i)}$ that $\sum_{i=1}^{N_t} F^{(i)} = \sum_{j=1}^{R_{N_t}} f(\Phi_j, \Phi_{j+1})$ and from the first corollary of the Ergodic Theorem (Bremaud, 2001, 3-Cor.4.1) which applies since f and π_{Φ} are bounded,

$$\frac{\mathbb{E}[F^{(i)}]}{\mathbb{E}[|\mathbf{X}^{(i)}|]} = \lim_{t \rightarrow \infty} \frac{\sum_{j=1}^{R_{N_t}} f(\Phi_j, \Phi_{j+1})}{R_{N_t}} \stackrel{a.s.}{=} \sum_{(u,v) \in \mathcal{V} \times \mathcal{V}} \pi_{\Phi}(u) p_{\Phi}(u,v) g(u,v) = \frac{2\mu(\mathcal{E})}{\text{Vol}(\mathcal{G})}.$$

From Kac's formula (Aldous and Fill, 2002, Cor.2.24) $1/\mathbb{E}[|\mathbf{X}^{(i)}|] = \pi_{\Phi}(x_0) = \frac{\mathbf{d}(x_0)}{\text{Vol}(\mathcal{G})}$. Therefore

$$\mathbb{E} \left[\frac{\mathbf{d}(x_0)}{2} F^{(i)} \right] \stackrel{a.s.}{=} \mu(\mathcal{E}).$$

The unbiasedness of $\hat{\mu}_*(\mathcal{T}; f, \mathcal{G})$ is seen by applying linearity of expectations on the summation over \mathcal{T} and consistency is a consequence of Kolmogorov's SLLN (Bremaud, 2001, 1-Thm.8.3). \square

Proof (Proof of Running Time) From Kac's formula (Aldous and Fill, 2002, Cor.2.24) $\mathbb{E}[|\mathbf{X}^{(i)}|] = \frac{\text{Vol}(\mathcal{G})}{\mathbf{d}(x_0)}$. From Proposition 8 we know that tours can be sampled independently and thus parallelly. In expectation an equal number of tours will be sampled on all cores yielding the expected running time bound. \square

Proof (Proof of Variance) The variance of the estimate is given by

$$\text{Var}(\hat{\mu}_*(\mathcal{T})) = \text{Var}\left(\frac{\mathbf{d}(x_0)}{2m} \sum_{\mathbf{x} \in \mathcal{T}} \sum_{j=1}^{|\mathbf{x}|} f(X_j, X_{j+1})\right) \leq \frac{\mathbf{d}(x_0)^2 B^2}{4m} \text{Var}(|\mathbf{x}|)$$

where B is the upper bound of f and the independence of tours is used. From Lemma 3 and Kac's formula (Aldous and Fill, 2002, Cor.2.24) we have

$$\text{Var}(|\mathbf{x}|) \leq \frac{3}{\pi_{\Phi}(x_0)^2 \delta(\Phi)} - \frac{1}{\pi_{\Phi}(x_0)^2} \leq \frac{3}{\pi_{\Phi}(x_0)^2 \delta(\Phi)}.$$

Combining the above two equations completes the proof. \square

C Proofs for Section 3

C.1 Proof of Proposition 1

Proof If we assume that Proposition 1 (a) doesn't hold, there exists a component such that the minimum value of ρ in that component is $\tilde{r} > 0$. In the graph stratum $\mathcal{G}_{\tilde{r}}$ (Definition 5), the supernode $\zeta_{\tilde{r}}$ will be disconnected all vertices in the above component. Therefore Proposition 1 (a) is necessary. Similarly, if Item Proposition 1 (b) is violated, a vertex \tilde{u} exists which is disconnected in $\mathcal{G}_{\rho(\tilde{u})}$ and if Item Proposition 1 (c) is violated, the supernode is disconnected.

When all three conditions hold it is trivial to see based on the above arguments that each stratum is connected and the partition is an *EPS*. \square

C.2 Proof of Proposition 2

Proof The proof is a direct consequence of Definition 5 and Definition 1. \square

C.3 Proof of Proposition 3

Proof Define $f' : \mathcal{E}_r \rightarrow \mathbb{R}$ as $f'(u, v) \triangleq \mathbf{1}\{u, v \neq \zeta_r\} f(u, v)$. By Definition 2, in each *RWT* $\mathbf{X} \in \mathcal{T}_r$, $f'(X_1, X_2) = f'(X_{|\mathbf{X}|}, X_{|\mathbf{X}|+1}) = 0$ and therefore

$$\hat{\mu}(\mathcal{T}_r; f, \mathcal{G}_r) = \hat{\mu}_*(\mathcal{T}; f', \mathcal{G}_r),$$

where $\hat{\mu}_*$ is the *RWT* Estimate From Lemma 1. Since \mathcal{G}_r is a graph stratum derived from an Ergodicity-Preserving Stratification, it is connected. Applying Lemma 1

$$\mathbb{E}[\hat{\mu}(\mathcal{T}_r; f, \mathcal{G}_r)] = \mathbb{E}[\hat{\mu}_*(\mathcal{T}; f', \mathcal{G}_r)] = \sum_{(u,v) \in \mathcal{E}_r} f'(u, v) = \sum_{(u,v) \in \mathcal{J}_r} f(u, v),$$

where the final equality is due to the observation made after Definition 5 where \mathcal{E}_r is the union of \mathcal{J}_r and edges which are incident on the supernode. Consistency is also due to Lemma 1 \square

C.4 Proof of Theorem 1

We begin by defining the multi-set containing the end points of edges between vertex strata.

Definition 13 Given a graph \mathcal{G} stratified into R strata, for all $1 \leq q < t \leq R$ define we define the border multi-sets as

$$\mathcal{B}_{q,t} \triangleq \{v \mid \forall (u,v) \in \mathcal{E} : u \in \mathcal{I}_q \text{ and } v \in \mathcal{I}_t\}.$$

Remark 6 Given Definition 13, the degree of the supernode in the r -th graph stratum \mathcal{G}_r is given by $\mathbf{d}(\zeta_r) = \sum_{q=1}^{r-1} |\mathcal{B}_{q,r}|$ and a the random walk transition probability out of ζ_r can be sampled by sampling $q \in \{1, \dots, r-1\}$ w.p. proportional to $|\mathcal{B}_{q,r}|$ and then by uniformly sampling from $\mathcal{B}_{q,r}$.

Proposition 9 *Given the setting in Definitions 8 and 9, for all $1 \leq r < t \leq R$,*

$$\lim_{|\mathcal{T}_2^\dagger| \rightarrow \infty} \dots \lim_{|\mathcal{T}_r^\dagger| \rightarrow \infty} \widehat{\beta}_{r,t} \stackrel{a.s.}{=} |\mathcal{B}_{r,t}|, \quad (17)$$

$$\lim_{|\mathcal{T}_2^\dagger| \rightarrow \infty} \dots \lim_{|\mathcal{T}_r^\dagger| \rightarrow \infty} \widehat{\mathbf{U}}_{r,t} \sim \text{UNIF}(\mathcal{B}_{r,t}). \quad (18)$$

and each tour \mathcal{T}_r^\dagger are perfectly sampled from Φ_r , i.e.

$$\lim_{|\mathcal{T}_2^\dagger| \rightarrow \infty} \dots \lim_{|\mathcal{T}_r^\dagger| \rightarrow \infty} p_{\Phi_r}(\mathbf{X}) = p_{\Phi_r}(\mathbf{X}), \quad \forall \mathbf{X} \in \mathcal{T}_r^\dagger. \quad (19)$$

Proof We prove Proposition 9 by strong induction. The base case for $r = 1$ holds by Definition 8. We now assume that Proposition 9 holds for all strata upto and including $r - 1$. All the following statements are under the limit $\lim_{|\mathcal{T}_2^\dagger| \rightarrow \infty} \dots \lim_{|\mathcal{T}_{r-1}^\dagger| \rightarrow \infty}$

We have,

$$\widehat{\mathbf{d}}(\zeta_r) = \sum_{q=1}^{r-1} \widehat{\beta}_{q,r} \stackrel{a.s.}{=} \sum_{q=1}^{r-1} |\mathcal{B}_{q,r}| = \mathbf{d}(\zeta_r),$$

where the almost sure convergence is due to the inductive claim and the next equality is by Remark 6. Moreover

$$\widehat{p}_{\Phi_r}(\zeta_r, \cdot) \equiv p_{\Phi_r}(\zeta_r, \cdot)$$

since the inductive claim makes the procedure of sampling a transition out of ζ_r in Definition 8 equivalent to the procedure in Remark 6. Therefore Equation (19) holds since the transition probabilities at all states other than ζ_r are equivalent in Φ_r and $\widehat{\Phi}_r$ according to Definition 7.

Recall that

$$\widehat{\beta}_{r,t} = \frac{\widehat{\mathbf{d}}(\zeta_r)}{|\mathcal{T}_r^\dagger|} \sum_{\mathbf{x} \in \mathcal{T}_r^\dagger} \sum_{j=2}^{|\mathbf{x}|} \mathbf{1}\{\rho(X_j) = t\}.$$

Since $\widehat{\mathbf{d}}(\zeta_r) = \mathbf{d}(\zeta_r)$ and the tours are sampled perfectly,

$$\widehat{\beta}_{r,t} = \hat{\mu}_* \left(\mathcal{T}_r^\dagger; f' \right),$$

where $f'(u, v) = \mathbf{1}\{\rho(v) = t\}$. Lemma 1 applies since \mathcal{G}_r is connected by Definition 6 and the consistency guarantee yields

$$\lim_{|\mathcal{T}_2^\dagger| \rightarrow \infty} \dots \lim_{|\mathcal{T}_r^\dagger| \rightarrow \infty} \widehat{\beta}_{r,t} \stackrel{a.s.}{=} \sum_{(u,v) \in \mathcal{E}_r} f'(u, v) = |\mathcal{B}_{r,t}|,$$

which proves Equation (17).

Now from Proposition 8 we know that concatenating tours $\mathbf{X} \in \mathcal{T}_q^\dagger$ yields a sample path from Φ_r . These samples will be distributed in according to π_{Φ_r} as $|\mathcal{T}_r^\dagger| \rightarrow \infty$. Therefore

$$\lim_{|\mathcal{T}_2^\dagger| \rightarrow \infty} \dots \lim_{|\mathcal{T}_r^\dagger| \rightarrow \infty} \mathbb{P}_{\mathbf{X} \in \mathcal{T}_q^\dagger}^{\mathbb{P}_{j=2}^{|\mathbf{X}|}} \{X_j : \rho(X_j) = t\} \sim \pi'_{\Phi_r},$$

where $\pi'_{\Phi_r}(u) \propto \mathbf{1}\{\rho(u) = t\} \mathbf{d}_{\mathcal{G}_r}(u)$ which is equivalent to $\text{UNIF}(\mathcal{B}_{r,t})$ by Definitions 5 and 13, thus proving Equation (18). \square

Theorem 1 is a direct consequence of applying Proposition 9 and Proposition 3.

C.5 Proof of Theorem 2

Definition 14 (L^2 distance between $\hat{\pi}$ and π (Aldous and Fill, 2002)) The L^2 distance between discrete probability distribution $\hat{\pi}$ and reference distribution π with sample space Ω is given by

$$\|\hat{\pi} - \pi\|_2 = \sum_{i \in \Omega} \frac{(\hat{\pi}(i) - \pi(i))^2}{\pi(i)}.$$

Definition 15 (Distorted chain) Given a Markov chain Φ over finite state space \mathcal{S} and an arbitrary $x_0 \in \mathcal{S}$, let $\hat{\Phi}$ be the distorted chain such that $\forall u \neq x_0, p_{\hat{\Phi}}(u, \cdot) = p_{\Phi}(u, \cdot)$ and $p_{\hat{\Phi}}(x_0, \cdot)$ is an arbitrary distribution with support such that $\text{supp}(p_{\hat{\Phi}}(x_0, \cdot)) \subseteq \text{supp}(p_{\Phi}(x_0, \cdot))$. The distortion is given by $\|p_{\hat{\Phi}}(x_0, \cdot) - p_{\Phi}(x_0, \cdot)\|$ as defined in Definition 14.

Lemma 4 Given a finite state, positive recurrent Markov chain Φ over state space \mathcal{S} . Let $\hat{\Phi}$ be the chain distorted at some $x_0 \in \mathcal{S}$ from Definition 15. Let

$$\mathcal{X} = \{(X_1, \dots, X_\xi) : X_1 = x_0, \xi = \min\{t > 0 : X_{t+1} = x_0\}, p_{\Phi}(X_1, \dots, X_\xi) > 0\},$$

denote the set of all possible arbitrary length RWTs that begin and end at x_0 from Definition 2. Given a tour $\mathbf{Y} \in \mathcal{X}$ sampled from Φ ,

$$\mathbb{E}_{\Phi} \left[\frac{p_{\hat{\Phi}}(Y_1, Y_2)}{p_{\Phi}(Y_1, Y_2)} F(\mathbf{Y}) \right] = \mathbb{E}_{\hat{\Phi}} [F(\mathbf{Y})], \quad (20)$$

where $F : \mathcal{X} \rightarrow \mathbb{R}$ is a bounded function, \mathbb{E}_{Φ} is the expectation under the distribution of tours sampled from the Markov chain Φ and $\mathbb{E}_{\hat{\Phi}}$ is similarly defined.

Proof All tours in \mathcal{X} are finite length due to the positive recurrence of Φ . The ratio of the probability of sampling the tour $\mathbf{Y} = (Y_1, \dots, Y_{\xi'})$ from the Markov chain $\hat{\Phi}$ to Φ is given by

$$\frac{p_{\hat{\Phi}}(\mathbf{Y})}{p_{\Phi}(\mathbf{Y})} = \frac{\prod_{j=1}^{\xi'} p_{\hat{\Phi}}(Y_j, Y_{j+1})}{\prod_{j=1}^{\xi'} p_{\Phi}(Y_j, Y_{j+1})} = \frac{p_{\hat{\Phi}}(Y_1, Y_2)}{p_{\Phi}(Y_1, Y_2)}, \quad (21)$$

since $p_{\Phi}(Y_j, \cdot) = p_{\hat{\Phi}}(Y_j, \cdot)$, $\forall 1 < j \leq \xi'$ because $Y_j \neq x_0$ by the definitions of \mathcal{X} and $\hat{\Phi}$.

Since $\text{supp}(p_{\hat{\Phi}}(x_0, \cdot)) \subseteq \text{supp}(p_{\Phi}(x_0, \cdot))$, $\text{supp}(p_{\hat{\Phi}}(\mathbf{Y})) \subseteq \text{supp}(p_{\Phi}(\mathbf{Y}))$. The theorem statement therefore directly draws from the definition of importance sampling (Robert and Casella, 2013, Def 3.9) with the importance weights derived in Equation (21). \square

Lemma 5 Given a simple random walk Φ on the connected non bipartite graph \mathcal{G} from Definition 1, let $\hat{\Phi}$ be the chain distorted at some $x_0 \in \mathcal{S}$ from with distortion ν Definition 15. Let $\lambda = \hat{\mathbf{d}}(x_0)/\mathbf{d}(x_0)$. Let $f : \mathcal{E} \rightarrow \mathbb{R}$ bounded by B , and $F(\mathbf{X}) = \sum_{j=1}^{|\mathbf{X}|} f(X_j, X_{j+1})$ where \mathbf{X} is an RWT as defined in Appendix B.1. The bias of an RWT Estimate (Equation (2)) computed using tours sampled over $\hat{\Phi}$ and using $\hat{\mathbf{d}}(x_0)$ as the degree is given by

$$\text{BIAS} = \left| \mathbb{E}_{\hat{\Phi}} \left[\frac{\hat{\mathbf{d}}(x_0)}{2} F(\mathbf{X}) \right] - \mu(\mathcal{E}) \right| \leq (\lambda\nu + |1 - \lambda|) \frac{\sqrt{3B}|\mathcal{E}|}{\sqrt{\delta}},$$

where δ is the spectral gap of Φ and B is the upper bound of f .

Proof From Lemma 4,

$$\mathbb{E}_{\hat{\Phi}} \left[\frac{\hat{\mathbf{d}}(x_0)}{2} F(\mathbf{X}) \right] = \mathbb{E}_{\Phi} \left[\frac{\hat{\mathbf{d}}(x_0)}{2} \frac{p_{\hat{\Phi}}(X_1, X_2)}{p_{\Phi}(X_1, X_2)} F(\mathbf{X}) \right].$$

Since from Lemma 1,

$$\mu(\mathcal{E}) = \mathbb{E}_{\Phi} \left[\frac{\mathbf{d}(x_0)}{2} F(\mathbf{X}) \right],$$

subtracting the two yields

$$\text{BIAS} = \mathbb{E}_{\Phi} \left[\left(\frac{\hat{\mathbf{d}}(x_0)}{\mathbf{d}(x_0)} \frac{p_{\hat{\Phi}}(X_1, X_2)}{p_{\Phi}(X_1, X_2)} - 1 \right) \frac{\mathbf{d}(x_0)}{2} F(\mathbf{X}) \right].$$

Squaring both sides and using the Cauchy-Schwarz inequality can decompose the squared bias as

$$\text{BIAS}^2 \leq \underbrace{\mathbb{E} \left[\left(\frac{\hat{\mathbf{d}}(x_0)}{\mathbf{d}(x_0)} \frac{p_{\hat{\Phi}}(x_0, X_2)}{p_{\Phi}(x_0, X_2)} - 1 \right)^2 \right]}_{\text{BIAS}_{\text{dist}}} \underbrace{\mathbb{E} \left[\left(\frac{\mathbf{d}(x_0)}{2} F(\mathbf{X}) \right)^2 \right]}_{\text{BIAS}_{\text{spectral}}},$$

where the expectation is under Φ .

Using definitions from the theorem statement,

$$\begin{aligned} \text{BIAS}_{\text{dist}} &= \frac{\hat{\mathbf{d}}(x_0)^2}{\mathbf{d}(x_0)^2} \mathbb{E} \left[\left(\frac{p_{\hat{\Phi}}(x_0, X_2)}{p_{\Phi}(x_0, X_2)} \right)^2 \right] + 1 - 2 \frac{\hat{\mathbf{d}}(x_0)}{\mathbf{d}(x_0)} \mathbb{E} \left[\frac{p_{\hat{\Phi}}(x_0, X_2)}{p_{\Phi}(x_0, X_2)} \right] \\ &= \lambda^2(1 + \nu^2) + 1 - 2\lambda = \lambda^2 + \lambda^2\nu^2 + 1 - 2\lambda \\ &= \lambda^2\nu^2 + (1 - \lambda)^2 \leq (\lambda\nu + |1 - \lambda|)^2. \end{aligned}$$

Since $F(\mathbf{X}) \leq B\xi$, the tour length, from Lemma 3 we see that

$$\text{BIAS}_{\text{spectral}} \leq \frac{\mathbf{d}(x_0)^2 B^2}{4} \frac{3}{\pi_{\Phi}(x_0)^2 \delta} = \frac{3B^2|\mathcal{E}|^2}{\delta},$$

and combining both biases completes the proof for BIAS. \square

Proof (Proof of the main theorem) Note that

$$\begin{aligned} \mathbb{E} \left[\hat{\mu}(\mathcal{T}_{2:r}^\dagger; f) \mid \mathcal{T}_{2:r-1}^\dagger \right] &= \mathbb{E} \left[\frac{\hat{\mathbf{d}}(\zeta_r)}{2|\mathcal{T}_r^\dagger|} \sum_{\mathbf{X} \in \mathcal{T}_r^\dagger} \sum_{j=2}^{|\mathbf{X}|-1} f(X_j, X_{j+1}) \right], \\ &= \mathbb{E}_{\mathbf{X} \sim \hat{\Phi}_r} \left[\frac{\hat{\mathbf{d}}(\zeta_r)}{2} \sum_{j=1}^{|\mathbf{X}|} f'(X_j, X_{j+1}) \right], \end{aligned}$$

by linearity of expectations, where \mathbf{X} is an *RWT* sampled on $\hat{\Phi}_r$ which depends on $\mathcal{T}_{2:r-1}^\dagger$ and $f'(u, v) \triangleq \mathbf{1}\{u, v \neq \zeta_r\} f(u, v)$. Applying Lemma 5 completes the proof since $\hat{\Phi}_r$ is a distorted chain by Definition 15. \square

D Proofs for Section 4

D.1 Proof of Proposition 4

Proof From Wang et al. (2014, Thm-3.1) we know that each disconnected component of G will lead to a disconnected component in $\mathcal{G}^{(k-1)}$ and if \mathcal{I}_1 contains a subgraph in each

connected component, Proposition 1 (a) is satisfied. We will now prove that for each $s \in \mathcal{V}^{(k-1)}$, if $\rho(s) = r > 1$, there exists $s' \in \mathbf{N}(s)$ such that $\rho(s') < r$ which simultaneously satisfies Proposition 1 (b) and Proposition 1 (c).

W.l.o.g let the vertex with the smallest distance from the seed vertices be denoted by $\hat{u} = \operatorname{argmin}_{u \in V(s)} \operatorname{DIST}(u)$.

When $\operatorname{DIST}(\hat{u}) > 0$, there exists $v \in \mathbf{N}_G(\hat{u})$ such that $\operatorname{DIST}(v) < \operatorname{DIST}(\hat{u})$ by the definition of DIST . More concretely v would be the penultimate vertex in the shortest path from the seed vertices to \hat{u} . Let $v' \neq \hat{u}$ be a non articulating vertex of s , which is possible since any connected graph has at least 2 non articulating vertices. Let $s_1 = G(V(s) \setminus \{v'\} \cup \{v\}) \in \mathcal{V}^{(k-1)}$. Now $\rho(s_1) < \rho(s)$ since v' has been replaced with a vertex necessarily smaller distance and since the indicator in the definition of ρ will always be 0 in this case. Moreover $s_1 \circ s = G(V(s) \cup \{v\}) \in \mathcal{V}^{(k)}$ and hence an edge exists between the two.

When $\operatorname{DIST}(\hat{u}) = 0$, there exists $v \in \mathbf{N}_G(\hat{u})$ such that $\operatorname{DIST}(v) = 0$. There exists a non articulating $v' \in V(s) \setminus V^*$ because otherwise V^* would have been disconnected. Observing that $\operatorname{DIST}(v') + \mathbf{1}\{v' \in V(\mathcal{I}_1) \setminus V^*\} > 0$ completes the proof of ergodicity. \square

D.1.1 Proof of Proposition 5

Proof (Sampling Probability) Consider the lines Lines 4 to 6. The probability of sampling the pair (u, v) from $V(s) \times \mathbf{N}_G(V(s))$ is given by

$$\begin{aligned} P(u, v) &= \sum_{a \in V(s) \setminus \{u\}} P(v|a, u) P(a|u) P(u) \\ &= \sum_{a \in V(s) \setminus \{u\}} \frac{\mathbf{1}\{v \in \mathbf{N}(a)\}}{\mathbf{d}(a)} \frac{\mathbf{d}(a)}{\deg_s - \mathbf{d}(u)} \frac{\deg_s - \mathbf{d}(u)}{(k-1-1)\deg_s} \\ &\propto \sum_{a \in V(s) \setminus \{u\}} \mathbf{1}\{v \in \mathbf{N}(a)\} = |N(v) \cap V(s) \setminus \{u\}| = \text{BIAS}, \end{aligned}$$

where BIAS is defined in Line 7 and corrected for in Line 8. Post the rejection therefore $(u, v) \sim \text{UNIF}(V(s) \times \mathbf{N}_G(V(s)))$.

Line 10 constitutes an importance sampling with unit weight for pairs (u, v) where removing u from and adding v to $V(s)$ produces a $k-1$ -CIS and zero otherwise. In Line 10, since removing a non-articulating vertex and adding another vertex to s cannot lead to a disconnected subgraph we can avoid a DFS when $u \notin \mathcal{A}_s$. This completes the proof. \square

Proof (Time Complexity) Assuming access to a precomputed vector of degrees, the part upto Line 2 is $O(k-1)^2$. In each proposal, Lines 4 and 5 are $O(k-1)$ and Line 6 is $O(\Delta_s)$. Line 7 is $O(k-1)$ and the expected complexity of Line 10 is $O(k-1^2 |\mathcal{A}_s| / (k-1))$ since in expectation only $|\mathcal{A}_s| / (k-1)$ graph traversals will be required. The acceptance probability is $\geq 1/(k-1)$ in Line 8 and $\geq \frac{k-1-|\mathcal{A}_s|}{k-1}$. The expected number of proposals is therefore $\leq \frac{k-1^2}{k-1-|\mathcal{A}_s|}$. As such the expected time complexity is $O(k-1^2(1 + \frac{\Delta_s + k-1-|\mathcal{A}_s|}{k-1-|\mathcal{A}_s|}))$. \square

D.2 Proof of Proposition 6

Lemma 6 *Given a stratification which yields the graph stratum \mathcal{G}_r from Definition 5, for some $r > 1$, define $\alpha_r = |\{u \in \mathcal{I}_r : \mathbf{N}(u) \cap \mathcal{I}_{1:r-1} \neq \emptyset\}| / |\mathcal{I}_r|$ as the fraction of vertices in the r -th vertex stratum which share an edge with a previous stratum. Let ξ_r be the return time of the random walker Φ_r to the supernode $\zeta_r \in \mathcal{V}_r$. Then*

$$\mathbb{E}_{\Phi_r}[\xi_r] \leq \frac{2\bar{\mathbf{d}}_r}{\alpha_r},$$

where $\bar{\mathbf{d}}_r$ is the average degree in \mathcal{G} of all vertices in \mathcal{I}_r .

Proof Since $\alpha_r \mathcal{I}_r$ vertices have at least one edge incident on ζ_r , $\mathbf{d}_{\mathcal{G}_r}(\zeta_r) \geq \alpha_r \mathcal{I}_r$. From Definition 5, since all edges not incident on \mathcal{I}_r are removed from \mathcal{G}_r , $\text{Vol}(\mathcal{G}_r) \leq 2 \sum_{u \in \mathcal{I}_r} \mathbf{d}_{\mathcal{G}}(u)$. Therefore, from Lemma 1,

$$\mathbb{E}_{\Phi_r}[\xi_r] = \frac{\text{Vol}(\mathcal{G}_r)}{\mathbf{d}(\zeta_r)} \leq \frac{2 \sum_{u \in \mathcal{I}_r} \mathbf{d}_{\mathcal{G}}(u)}{\alpha_r \mathcal{I}_r} = \frac{2\mathbf{d}_r}{\alpha_r}.$$

□

Proposition 10 *The Ergodicity-Preserving Stratification from Proposition 4 is such that $\alpha_r = 1$ for all $r > 1$ as defined in Lemma 6, and consequently the diameter of each graph stratum is ≤ 4 . The total number of strata $R \in O(k D_G)$, the diameter of G .*

Proof We show in Appendix D.1 that for each vertex $s \in \mathcal{V}^{(k-1)}$, if $\rho(s) = r > 1$, there exists $s' \in \mathbf{N}(s)$ such that $\rho(s') < r$. This implies that $\alpha_r = 1$. In \mathcal{G}_r therefore, from ζ_r , all vertices in \mathcal{I}_r are at unit distance from ζ_r and vertices in $\mathbf{N}(\mathcal{I}_r) \setminus \mathcal{I}_r$ are at a distance of 2 from ζ_r . Since no other vertices are present in \mathcal{G}_r this completes the proof of the first part. Trivially, $R \leq (k-1) \cdot \max_{u \in V} \text{DIST}(u) \in O(k \cdot D_G)$. □

Proof (Proof of Memory Complexity) As apparent from Algorithm 2, we compute a single count estimate, per stratum and maintain reservoirs and inter-partition edge count estimates for each $2 \leq q < t \leq R$. Since each reservoir $\hat{\mathbf{U}}_{q,t}$, needs $O(km)$ space based on the discussion in Section 4.3, the total memory requirement is $O(R^2 km)$, where R is the number of strata. Since by Proposition 10 $R \in O(k D_G)$, the total memory requirement is $O((k D_G)^2 km)$.

The $|\mathcal{H}|$ extra memory is to store the output $\hat{\mu}$. □

Proof (Proof of Time Complexity) From Section 4.2 the stratification procedure requires a single BFS which is $O(|V| + |E|)$.

In Line 3 the estimation phase starts by iterating over the entire higher order neighborhood of each subgraphs in \mathcal{I}_1 . In Remark 5 we show that the complexity of computing Line 5 is $O(k^2)$. Since the size of the higher order neighborhood of each subgraph is $O(k^2 \Delta_G)$ based on the discussion after Equation (11), the initial estimation phase will require $O(|\mathcal{I}_1| k^2 \Delta_G k^2) \equiv O(|\mathcal{I}_1| k^4 \Delta_G)$ time.

In all other strata $r = 2, \dots, R$, we assume that m tours are sampled in Line 8. Starting each tour (Lines 9 to 11) requires order R time, therefore leading to a total time of $O(m R^2) \in O(m k^2 D_G^2)$ since $R \in O(k D_G)$ from Proposition 10. The total time for these ancillary procedures is $O(m k^2 D_G^2 + |\mathcal{I}_1| k^4 \Delta_G)$.

Therefore the time complexity of bookkeeping and setup is $O(m k^2 D_G^2 + |\mathcal{I}_1| k^4 \Delta_G + |V| + |E|) \in \tilde{O}(k^4)$. The time complexity at each random walk step is $O(k-1^2 \Delta_G + k-1^4) \in \tilde{O}(k^4)$ from Appendix D.1.1 and Remark 5.

We assume that the expected number of rejections in Line 21 is given by C_{REJ} . The total number of random walk steps is given by $O(R m C_{\text{REJ}})$ times the expected tour length. By Lemma 6 and proposition 10, the expected tour length is $O(\Delta_{\mathcal{G}^{(k-1)}}) \equiv O(k^2 \Delta_G)$. Therefore the total number of random walk steps is $O(k^3 m D_G \Delta_G C_{\text{REJ}})$.

The $|\mathcal{H}|$ extra time is to print the output $\hat{\mu}$. We assume that updating $\hat{\mu}$ is amortized constant order if we use a hashmap to store elements of the vector and since by Equation (10) increments involve updating a single key in said hashmap.

Combining these complexities completes the proof. □

E Additional Results

In this section we present the results of additional experiments performed on Ripple. Figure 8 shows the L2-norm from the ground truth for $k = 3$ with $m = 10^7$ while ϵ and \mathcal{I}_1 vary. Similarly Figure 9 shows the L2-norm as we vary the reservoir capacity m , for fixed $\epsilon = 0.003$ and $\mathcal{I}_1 = 10^7$.

In addition to Figure 6 showed in Section 5, we present evidence of convergence for $k \in \{6, 8, 10\}$ in Figure 10, Figure 11 and Figure 12 respectively. Similar to $k = 12$, we vary ϵ while setting $|\mathcal{I}_1| = 10^4$ and $m = 10^7$. In these figures we observe a behavior similar to the plots presented for $k = 12$ in Section 5, that is the estimates converge as ϵ reduces.

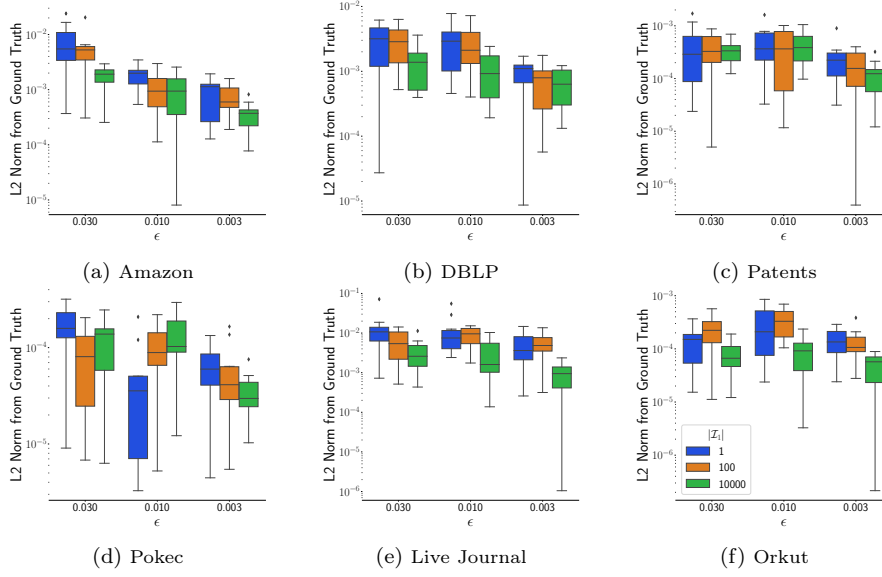


Fig. 8: Accuracy and convergence analysis for 3-CIS s. The y -axes show the L2-norm between the Ripple estimate and the ground truth vector $\mathcal{C}^{(k)}$ (Equation (10)) containing counts of all possible non isomorphic subgraph patterns while varying parameters ϵ and number of subgraphs in \mathcal{I}_1 . Each box and whisker represents 10 runs. Although we can see improvements as \mathcal{I}_1 is increased and ϵ is decreased, the effect is not as significant as for $k = 5$ (Figure 4). The differences between the results for $k = 3$ and 5 are explained by the subgraph space sizes where the former is orders-of-magnitude smaller (see Section 5 – Table 1).

Scalability on number of threads (Figure 13). In these experiments we set $\epsilon = 0.001$, $|\mathcal{I}_1| = 10^4$ and $M = 10^7$. In order to have sufficient workload even when using less cores (e.g., 9 and 18) we fixed $k = 5$. We set $\epsilon = 0.001$ to force a larger number of tours (Remark 3), thereby increasing the load per core. Running times are computed over 10 executions and excludes the graph reading time which is not optimized. We observe that the scalability of our implementation is not linear: as we double the number of cores the running time decreases by around a quarter instead of half. Local profiling using hardware performance counters (Linux’s *perf*) suggests that the reason for this overhead to be an outcome of increased random-access patterns of in-memory graph data, which limits the overall utilization of the underlying processing pipeline. Indeed, sub-optimal access patterns of graph data is a known issue that is currently handled by dedicated accelerator hardware deploying optimized and specific caching mechanisms and memory access policies for workloads dominated by subgraph enumeration (Yao et al., 2020).

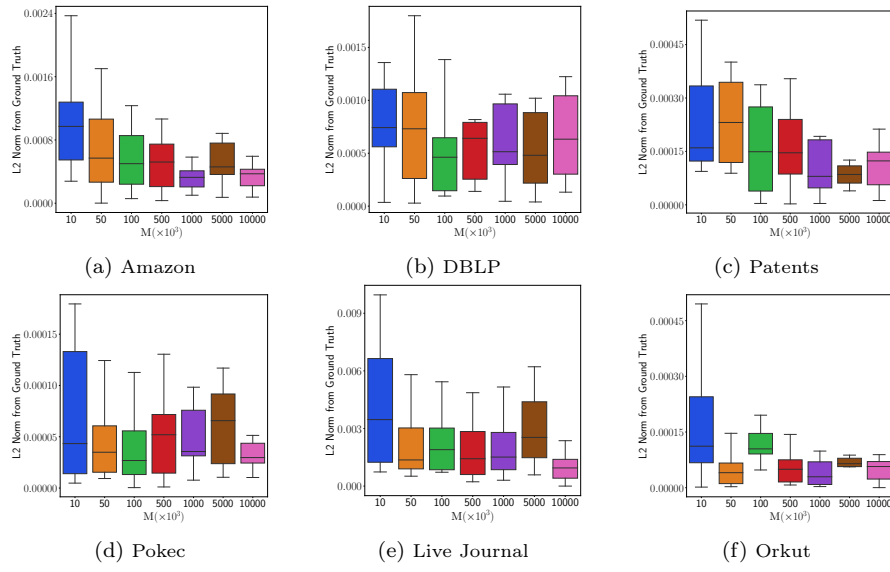


Fig. 9: Sensitivity of Ripple to the reservoir capacity M for $k = 3$. As in Figure 5, we verify through box and whiskers plots over 10 runs, that a larger reservoir improves the accuracy of Ripple estimates in all graphs since it reduces oversampling bias. In some networks like DBLB, the improvement is not apparent because Ripple converges to the ground truth very fast thereby requiring a very small M .

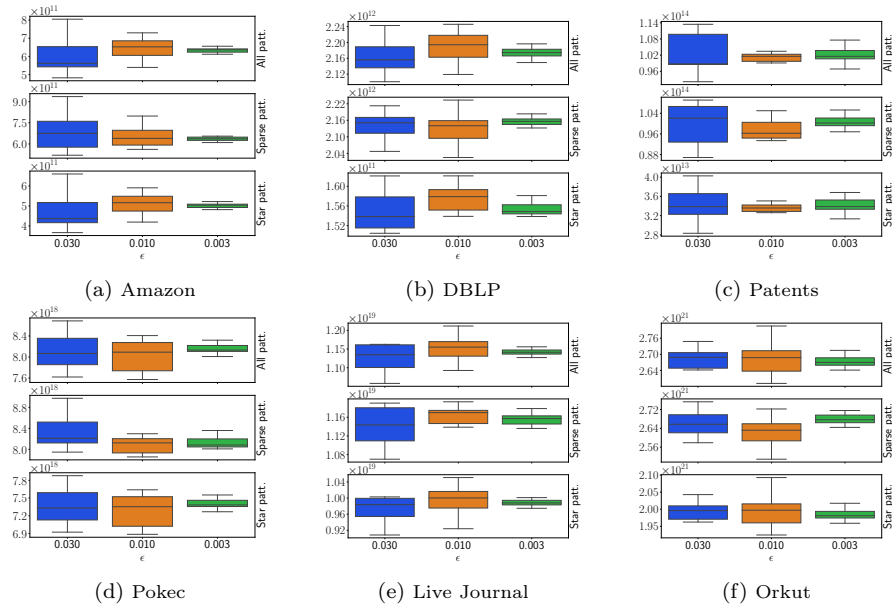


Fig. 10: Convergence of Ripple estimates of 6-CIS pattern counts. We estimate the total count of subgraphs $|\mathcal{V}^{(6)}|$, the number of sparse patterns and stars. The estimates over 10 runs are presented as box and whiskers plots which exhibit a reduction in variance as ϵ increases. Indeed, the Ripple estimates converge as we reduce ϵ .

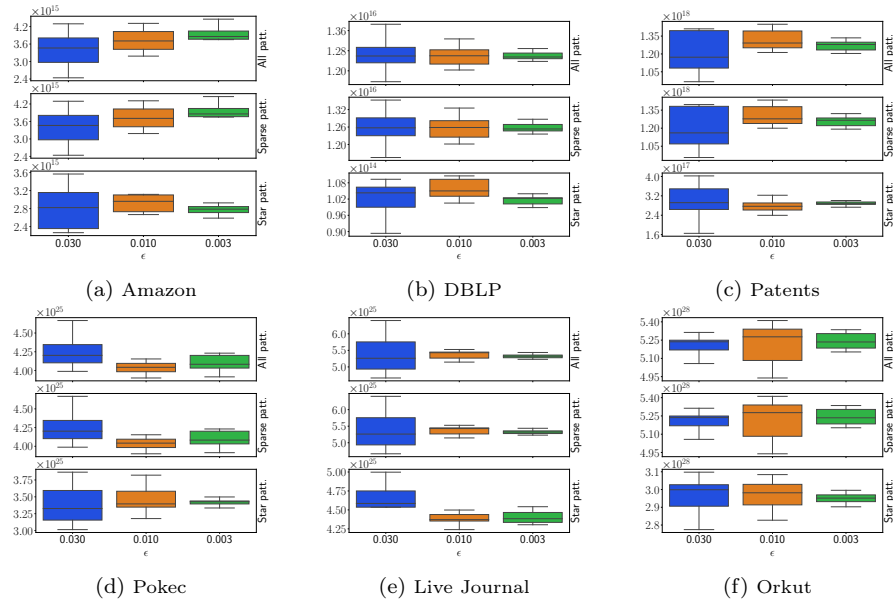


Fig. 11: Convergence of Ripple estimates of 8-CIS pattern counts. We estimate the total count of subgraphs $|\mathcal{V}^{(8)}|$, the number of sparse patterns and stars. The estimates over 10 runs are presented as box and whiskers plots which exhibit a reduction in variance as ϵ increases. Indeed, the Ripple estimates converge as we reduce ϵ .

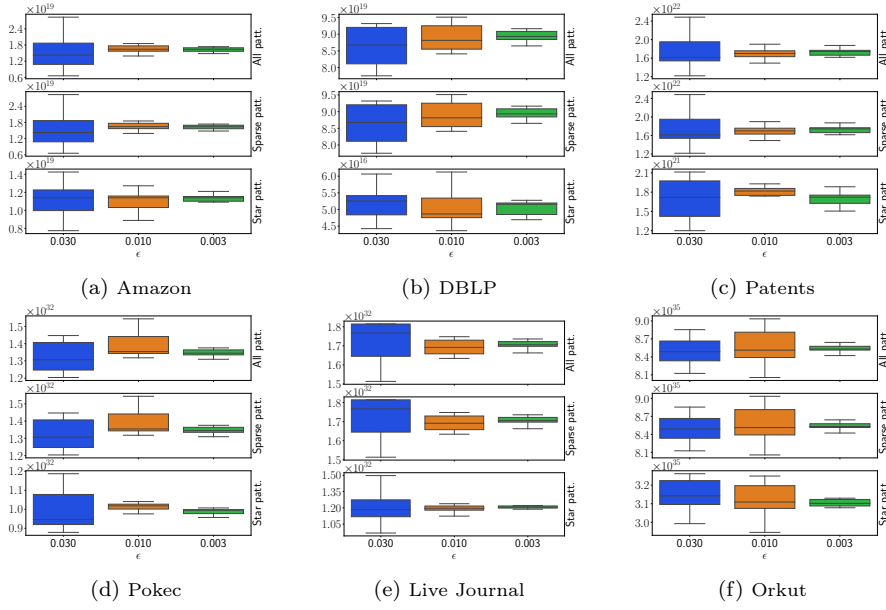


Fig. 12: Convergence of Ripple estimates of 10-*CIS* pattern counts. We estimate the total count of subgraphs $|\mathcal{V}^{(10)}|$, the number of sparse patterns and stars. The estimates over 10 runs are presented as box and whiskers plots which exhibit a reduction in variance as ϵ increases. Indeed, the Ripple estimates converge as we reduce ϵ .

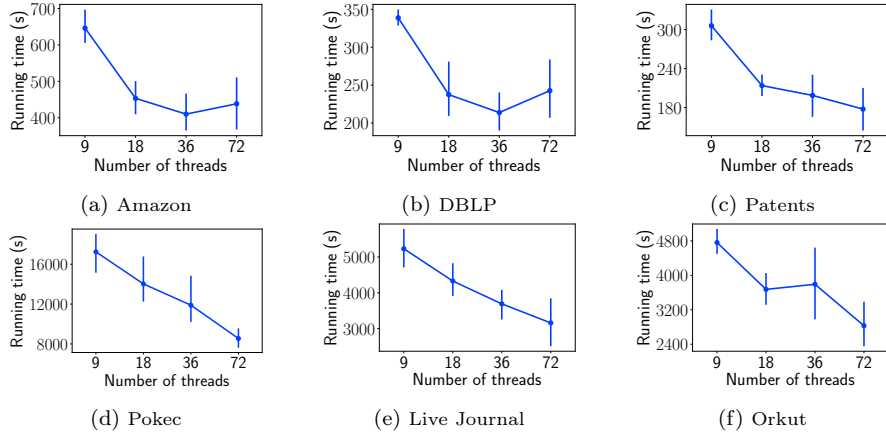


Fig. 13: Scalability with regards to the number of threads for 5-*CIS*. Despite a noticeable reduction in running time with more cores, we observe that the scalability is not linear. As we double the number of cores the running time decreases by about a quarter instead of half. This is due to the memory bandwidth limit coupled with the lack of (memory) locality ubiquitous in graph mining algorithms.